



Asynchronous Accumulation of Organic Carbon and Nitrogen in the Atlantic Gateway to the Arctic Ocean

Maria L. Paulsen^{1*}, Lena Seuthe², Marit Reigstad¹, Aud Larsen^{1,3}, Mattias R. Cape⁴ and Maria Vernet⁵

¹ Department of Biological Sciences, University of Bergen, Bergen, Norway, ² Department of Arctic and Marine Biology, University of Tromsø – The Arctic University of Norway, Tromsø, Norway, ³ NORCE Norwegian Research Centre AS, Bergen, Norway, ⁴ School of Oceanography, University of Washington, Seattle, WA, United States, ⁵ Scripps Institution of Oceanography, San Diego, CA, United States

OPEN ACCESS

Edited by:

Angel Borja,
Centro Tecnológico Experto en
Innovación Marina y Alimentaria
(AZTI), Spain

Reviewed by:

Urania Christaki,
Université du Littoral Côte d'Opale,
France
Philippe Massicotte,
Laval University, Canada

*Correspondence:

Maria L. Paulsen
marialundpaulsen@gmail.com

Specialty section:

This article was submitted to
Marine Ecosystem Ecology,
a section of the journal
Frontiers in Marine Science

Received: 28 June 2018

Accepted: 17 October 2018

Published: 15 November 2018

Citation:

Paulsen ML, Seuthe L,
Reigstad M, Larsen A, Cape MR and
Vernet M (2018) Asynchronous
Accumulation of Organic Carbon
and Nitrogen in the Atlantic Gateway
to the Arctic Ocean.
Front. Mar. Sci. 5:416.
doi: 10.3389/fmars.2018.00416

Nitrogen (N) is the main limiting nutrient for biological production in the Arctic Ocean. While dissolved inorganic N (DIN) is well studied, the substantial pool of N bound in organic matter (OM) and its bioavailability in the system is rarely considered. Covering a full annual cycle, we here follow N and carbon (C) content in particulate (P) and dissolved (D) OM within the Atlantic water inflow to the Arctic Ocean. While particulate organic carbon (POC), particulate organic nitrogen (PON), and dissolved organic carbon (DOC) accumulated in the surface waters from January to May, the dissolved organic nitrogen (DON)-pool decreased substantially ($\Delta - 50 \mu\text{g N L}^{-1}$). The DON reduction was greater than the simultaneous reduction in DIN ($\Delta - 30 \mu\text{g N L}^{-1}$), demonstrating that DON is a valuable N-source supporting the growing biomass. While the accumulating POM had a C/N ratio close to Redfield, the asynchronous accumulation of C and N in the dissolved pool resulted in a drastic increase in the C/N ratio of dissolved organic molecules (DOM) during the spring bloom. This is likely due to a combination of the reduction in DON, and a high release of carbon-rich sugars from phytoplankton, as 32% of the spring primary production (PP) was dissolved. Our findings thus caution calculations of particulate PP from DIN drawdown. During post-bloom the DON pool increased threefold due to an enhanced microbial processing of OM and reduced phytoplankton production. The light absorption spectra of DOM revealed high absorption within the UV range during spring bloom indicating DOM with low molecular weight in this period. The absorption of DOM was generally lower in the winter months than in spring and summer. Our results demonstrate that the change in ecosystem function (i.e., phytoplankton species and activity, bacterial activity and grazing) in different seasons is associated with strong changes in the C/N ratios and optical character of DOM and underpin the essential role of DON for the production cycle in the Arctic.

Keywords: particulate and dissolved organic matter, nitrogen pools, dissolved primary production, high latitude ecosystems, marginal ice zone, Svalbard, West Spitsbergen Current, microorganisms

INTRODUCTION

In the Arctic Ocean, productive shelf seas surround parts of the deep and less productive central basins (Sakshaug, 2004). The primary production (PP) is subject to a strong seasonal cycle in irradiance, as well as to a varying degree of sea ice cover. Sea ice can restrict PP due to shading but can also lead to enhanced PP by stabilizing the water column as it melts. In spring when the ice starts melting, intense phytoplankton blooms can be encountered along the retreating ice edge (Sakshaug and Skjoldal, 1989). Although seldom lasting for longer than 20 days (Perrette et al., 2011), these blooms can generate over 50% of the annual PP in the Arctic Ocean (Sakshaug, 2004) and are hence crucial in fuelling the arctic marine food web. For the less productive central Arctic Ocean, import of organic matter (OM) from its more productive adjacent shelf seas is suggested as an important marine carbon source to sustain its heterotrophic metabolism (Walsh et al., 1989; Wheeler et al., 1997; Shen et al., 2012). Both, the Chukchi (Wheeler et al., 1997; Bates et al., 2005; Davis and Benner, 2005; Mathis et al., 2007) and the Barents Sea (Fransson et al., 2001; Kivimae et al., 2010), are net exporters of organic carbon to the central Arctic Ocean, but the largest transporter of volume, heat and biomass is the West Spitsbergen Current (WSC) (Fahrbach et al., 2001; Shen et al., 2012). In order to understand the ecosystem of the Arctic Ocean it is therefore essential to understand what governs the production, transformation and export of OM and nutrients at the productive rim of the Arctic Ocean, especially within the Atlantic water inflow to the Arctic Ocean.

Microorganisms play a fundamental role in the cycling of organic carbon and nutrients. Through photosynthesis, microscopic marine phytoplankton fix inorganic carbon into OM. The photosynthetically produced OM does not only occur as phytoplankton cells (i.e., particulate form), but is also released by phytoplankton as dissolved organic molecules (DOM) through passive diffusion of low molecular compounds over the cell membrane (Bjørnson, 1988; Maranon et al., 2004) or by active excretion (Fogg, 1983; Mykkestad et al., 1989; Baines and Pace, 1991). The direct production of DOM by phytoplankton (PP_{diss}) can be a substantial fraction (up to 50%) of the gross PP and appears to be elevated especially in high latitude systems relative to temperate (Kirchman et al., 1991; Vernet et al., 1998). Further, the different species of phytoplankton produce photosynthate of different qualities. In the Arctic, for example, the bloom-forming prymnesiophyte *Phaeocystis pouchetii* produces copious amounts of neutral and acidic polysaccharides, which are released from exponentially growing cells, and can induce gel or transparent exopolymer particles (TEP) formation, in turn effectively promoting passive sinking (Le Moigne et al., 2015; Assmy et al., 2017; Engel et al., 2017).

The trophic fate of the photosynthetically fixed OM is different for particulate and dissolved forms. POM serves as food for phagotrophic (particle feeding) organisms of successively larger size and hence forms the basis for an effective energy transfer from the primary producers to higher trophic levels. During the transfer through the phagotrophic grazer food chain, parts of

POM are transferred to DOM, through sloppy feeding, excretion and defecation by phagotrophs (Jumars et al., 1989; Nagata and Kirchman, 1991; Strom et al., 1997). Viral lysis of bacteria (Middelboe et al., 1996) and phytoplankton (Bratbak et al., 1992; Agusti and Duarte, 2013) are additional DOM producing processes. The oceanic DOM pool thus originates from different autochthonous sources, both directly from the phytoplankton by PP_{diss}, and indirectly through the release of originally particulate matter through heterotrophic activities.

The process by which DOM is formed impacts its chemical composition and nutritional value for bacteria. DOM excreted by phytoplankton is often rich in carbohydrates (Ittekkot et al., 1981; Mykkestad, 1995), and can have high C/N ratio relative to the Redfield ratio (106:16 or 6.6) (Redfield, 1934, 1958), whereas DOM produced by trophic interactions is richer in nitrogen and consequently have C/N ratios closer to or below Redfield (Bronk et al., 1998; Saba et al., 2011). Generally, bacterial growth efficiency is higher when the C/N ratio of DOM is low, i.e., closer to their cellular C/N stoichiometry of 7.9 (Von Stockar and Liu, 1999), especially when inorganic N (DIN) sources are limiting (del Giorgio and Cole, 1998; Pradeep Ram et al., 2003). Labile DOM has a C/N stoichiometry of around 10, whereas the corresponding value for refractory DOM is 17.4 (Hopkinson and Vallino, 2005). Bacteria are likely to be net mineralizers of inorganic nutrients during degradation of labile DOM and net consumers of nutrients during degradation of substrates with a higher C/N stoichiometry (Goldman et al., 1987).

Primary productivity in the ocean is often limited by the availability of N. The productive surface layer of Arctic marine ecosystems is particularly low in DIN supply, as the concentrations of inorganic N in Arctic runoff are among the lowest worldwide (Dittmar and Kattner, 2003), there is little supply via N-fixating organisms (Sipler et al., 2017), and as strong stratification limits vertical mixing (Codispoti et al., 2013; Randelhoff et al., 2015). Therefore, Arctic Ocean phytoplankton blooms are mostly found to terminate with the depletion of nitrate (Popova et al., 2013; Tremblay et al., 2015). The current CO₂-enrichment of our atmosphere stimulates PP both on land (Reich et al., 2006) and in the ocean (Holding et al., 2015; Sanz-Martín et al., 2018). It is, therefore, speculated whether N-limitation could become more widespread in the future, especially in the Arctic where PP is also predicted to be stimulated by a longer ice-free season. This stresses the need to improve our understanding of how both phytoplankton and heterotrophic microorganisms affect the seasonal N-cycling in the region.

Here, we investigate (1) the link between biological processes and the partitioning of N-pools between DIN, dissolved organic nitrogen (DON), and PON during a full annual cycle and (2) the partitioning of particulate and dissolved PP during the spring bloom and post-bloom conditions, and how this influence the character and fate of the OM being produced. These observations are novel for the studied area and improve our knowledge on the interplay between biological processes and C/N stoichiometry of POM and DOM within the main Atlantic water inflow to the Arctic Ocean.

MATERIALS AND METHODS

General Sampling

The study was conducted on and off the shelf northwest of Svalbard (Figure 1) during cruises in January, March, May, August, and November 2014. The sampling concentrated on the core of the northwards drifting warm Atlantic water, which enters the Arctic Ocean north of Svalbard either south or north of the Yermak plateau. Heavy drift ice restricted the sampling to the shelf and shelf-break in May and August 2014. During January, March, and November, the area north of Svalbard was largely ice-free, which allowed sampling off the shelf-break into the Arctic Ocean during winter.

At all stations, depth profiles of temperature, salinity and fluorescence were taken with a CTD (Seabird SBE 911 plus). Water was sampled with Niskin bottles from discrete depths for analysis of inorganic nutrients, chlorophyll *a* (Chl *a*), microbial abundance, bacterial production (BP), as well as DOM and POM. In May and August, three stations were each sampled to investigate time-demanding processes, such as *in situ* PP and vertical export of POM. There are hereafter called “P-stations”: P1, P3, P4 in May (N.B. there is no P2 as moorings carrying PP incubations and sediment traps were lost), and P5, P6, P7 in August; see Figure 1 and Supplementary Table S1.

The sampling depths were 1, 5, 10, 20, 30, 50, 100, 200, 500, 750, and 1000 m. At stations on the shelf or shelf-edge with depths <1000 m, the deepest sample was taken close to the sea floor, and the sampling resolution close to the surface was increased by inserting additional sampling at 40 and 75 m, as well as at the depth of the Chl *a* maximum.

Chlorophyll *a* Concentration and Primary Production

Chl *a* ($\mu\text{g L}^{-1}$) was determined for two different size fractions by collecting suspended material onto Whatman GF/F, as well as membrane filters of 10 μm pore size (Whatman Nuclepore Track-Etch membrane). This allowed dividing the Chl *a* (determined from GF/F filters) into total and micro-size (>10 μm). Chl *a* was determined fluorometrically (10-AU, Turner Designs) from triplicates of each filter type after extraction in 5 mL methanol at room temperature in the dark for 12 h without grinding.

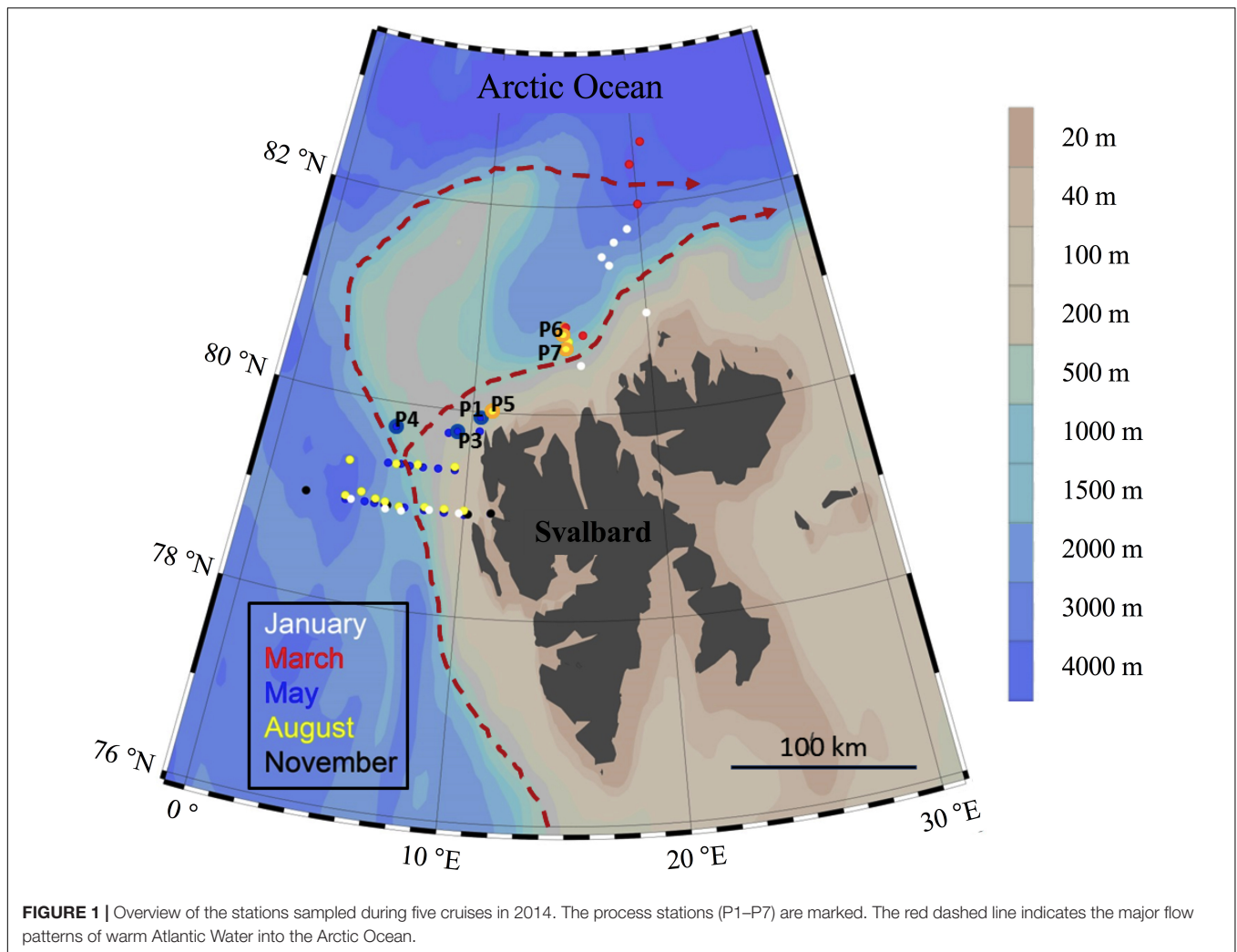
Water for PP measurements was collected from 0, 5, 10, 20, 30, 40, 50, and 75 m depth at all P-stations. The water from each depth was sampled and distributed in four 150 mL polycarbonate bottles; two light bottles and one dark bottle incubated *in situ* and one used as t_0 sample. 10 μCi of ^{14}C -labeled bicarbonate was dispensed into each bottle. The t_0 sample was immediately processed. For each depth, 100 mL were sampled onto a 6 mL scintillation vial containing 0.1 mL 6 N NaOH in order to estimate ^{14}C -bicarbonate concentration. The light and dark bottles were deployed at their respective sampling depths for approximately 22 h, using a mooring attached to an ice-float or drifting freely. At the end of the experiment, the bottles were recovered and sampled, keeping the bottles refrigerated. Light and dark bottles were treated equally: 0.2 mL of 20%

HCl was dispensed into each 6 mL scintillation vial containing either a Whatman GF/F filter (for PP_{part}) or 2 mL of seawater (for PP_{total}) in order to release any inorganic ^{14}C remaining in the sample. After 24 h, 5 mL of Ultima GoldTM XR LSC cocktail was added and the samples stored in the dark. On-shore, each vial was shaken and the ^{14}C activity measured in a Perkin Elmer scintillation counter (Tri-Carb 2900TR). PP was calculated by subtracting the activity in the dark bottle from the activity in the light bottles. Dissolved inorganic carbon (DIC) concentrations used for the calculation were measured by Melissa Cierci (pers. comm.) from total alkalinity and pH using the CO_2 -calculation program CO2SYS. For each depth, three PP estimates are provided, which are total primary production (PP_{total} , estimated from 2 mL water), particulate primary production (PP_{part} , estimated by filtering 98 mL water onto a Whatman GF/F filter), and dissolved primary production (PP_{diss} , which was calculated as $\text{PP}_{\text{total}} - \text{PP}_{\text{part}}$). The limit of detection is estimated at ca. 1 $\mu\text{g C L}^{-1} \text{d}^{-1}$. The percent dissolved PP (% PP_{diss}) was calculated as $100 \times (\text{PP}_{\text{diss}}/\text{PP}_{\text{total}})$.

Bacterial Production, Carbon Demand, and Microbial Abundance

At the P-stations, BP was estimated from incorporation rates of ^3H -labeled leucine (specific activity: 5.957 TBq mmol^{-1}), measured by standard methods (Kirchman, 2001). Triplicate water samples of 1.9 mL volume were incubated with ^3H -leucine (final conc. 20 nM) from each profile depth in the dark at 1°C for 2 h. The incubation was terminated by adding trichloroacetic acid (TCA; final conc. 5%). To account for potential passive adsorption of radioactivity, a TCA-killed control sample was incubated with ^3H -leucine together with the live samples from each depth. All samples were microcentrifuged to collect the incorporated ^3H -leucine and rinsed with TCA and ethanol. The samples were dried before radio assaying with liquid scintillation liquid (Ultima GoldTM XR LSC cocktail) in a scintillation counter (Perkin Elmer Tri-Carb 2900TR). Leucine incorporation was converted into biomass production using a carbon fraction of proteins of 1.5 (Simon and Azam, 1989; Ducklow, 2003), assuming no isotope dilution. The bacterial carbon demand (BCD) was estimated as the sum of BP and bacterial respiration (BR). BR was estimated from BP as $\text{BR} = 3.69 \times \text{BP}^{0.58}$, according to Robinson (2008). Specific bacterial growth rates were calculated by dividing BP by the bacterial abundance.

Abundances of heterotrophic bacteria and nanoflagellates (HNF) were determined on an Attune[®] Focusing Flow Cytometer (Applied Biosystems by Life technologies) with a syringe-based fluidic system and a 20 mW 488 nm (blue) laser. Samples were fixed with glutaraldehyde (0.5% final conc.) at 4°C for minimum 2 h, shock-frozen in liquid nitrogen, and stored at -80°C until analysis. For enumeration of B and V, the samples were diluted 10-fold with 0.2 μm filtered TE buffer (Tris 10 mM, EDTA 1 mM, pH 8), stained with a green fluorescent nucleic-acid dye, SYBR Green I (Molecular Probes Inc., Eugene, Oregon) by incubation for 10 min at $+80^\circ\text{C}$. Prior to HNF-enumeration, the samples were stained with SYBR Green I (Molecular Probes, Eugene, OR, United States) for 2 h in the dark. A minimum of 1 mL was



measured at a flow rate of $500 \mu\text{L min}^{-1}$ and the population was discriminated from nano-sized phytoplankton and large bacteria on basis of green vs. red fluorescence following the protocol of Zubkov et al. (2007).

Total, Particulate and Dissolved Organic Matter

Total organic carbon (TOC) in unfiltered seawater was analyzed by high-temperature combustion using a Shimadzu TOC-V_{CSH}. All samples were acidified with HCl (to a pH of around 2) and bubbled with pure N₂ gas in order to remove any inorganic carbon. Calibration was performed using deep seawater and low carbon reference waters. A blank consisting of milliQ water was analyzed every eighth sample to assess any day-to-day instrument variability. The concentration of total nitrogen (TN) was determined simultaneously by high-temperature combustion using a CPH-TN nitrogen analyser. Total organic nitrogen (TON) was calculated by subtracting the inorganic nitrogen (DIN = NO₃ + NO₂ + NH₄⁺) measured from parallel nutrient samples. The instrument was calibrated using a standard series of acetanilide and the accuracy of the

instrument was evaluated using seawater reference material provided by the Hansell CRM (consensus reference material) program.

For analysis of particulate organic carbon (POC) and particulate organic nitrogen (PON), triplicate subsamples (100–500 mL) were filtered onto pre-combusted Whatman GF/F glass-fiber filters (450°C for 5 h), dried at 60°C for 24 h and analyzed on-shore with a Leeman Lab CEC 440 CHN analyser. Prior to analysis, the dried samples were fumed by concentrated HCl for 24 h before re-drying at 60°C for 24 h to remove inorganic carbon.

The concentration of the DOM fractions was calculated as

$$\text{DOC} = \text{TOC} - \text{POC}$$

and

$$\text{DON} = \text{TN} - \text{DIN} - \text{PON}$$

Samples for NO₃⁻ and NO₂⁻ were stored frozen in acid-washed plastic bottles, and analyzed with standard seawater methods, applying Flow Solution IV analyser (OI Analytical) calibrated using reference seawater (Ocean Scientific

International). Samples for NH_4^+ were analyzed immediately upon sampling with the sensitive fluorometric method (Holmes et al., 1999). The sum of NO_3^- , NO_2^- , and NH_4^+ is called DIN hereafter.

Colored Dissolved Organic Matter (CDOM)

Samples for light absorption by colored DOM (CDOM) were taken directly from the Niskin bottles and filtered through $0.2 \mu\text{m}$ pore size filters (PALL Life Sciences IC Acrodisc® with Supor® membrane) into pre-combusted 30 mL amber glass vials using non-pyrogenic syringes. The samples were stored in dark at $+4^\circ\text{C}$ until analysis. The absorbance of CDOM was measured in the spectral range between 240 and 700 nm with an increment of 0.5 nm using a Shimadzu UV-2450 spectrophotometer and 10 cm quartz cells with ultrapure Milli-Q as a reference, following a procedure described in Stedmon and Markager (2001). The following spectrophotometer settings were used: slit width of 5 nm and fast scan speed. Absorbance values were baseline corrected by MQ blanks and then converted to an absorption coefficient [$a_{\text{CDOM}}(\lambda)$ with m^{-1} as unit] following:

$$a_{\text{CDOM}}(\lambda) = 2.303 \cdot A(\lambda) / l + K,$$

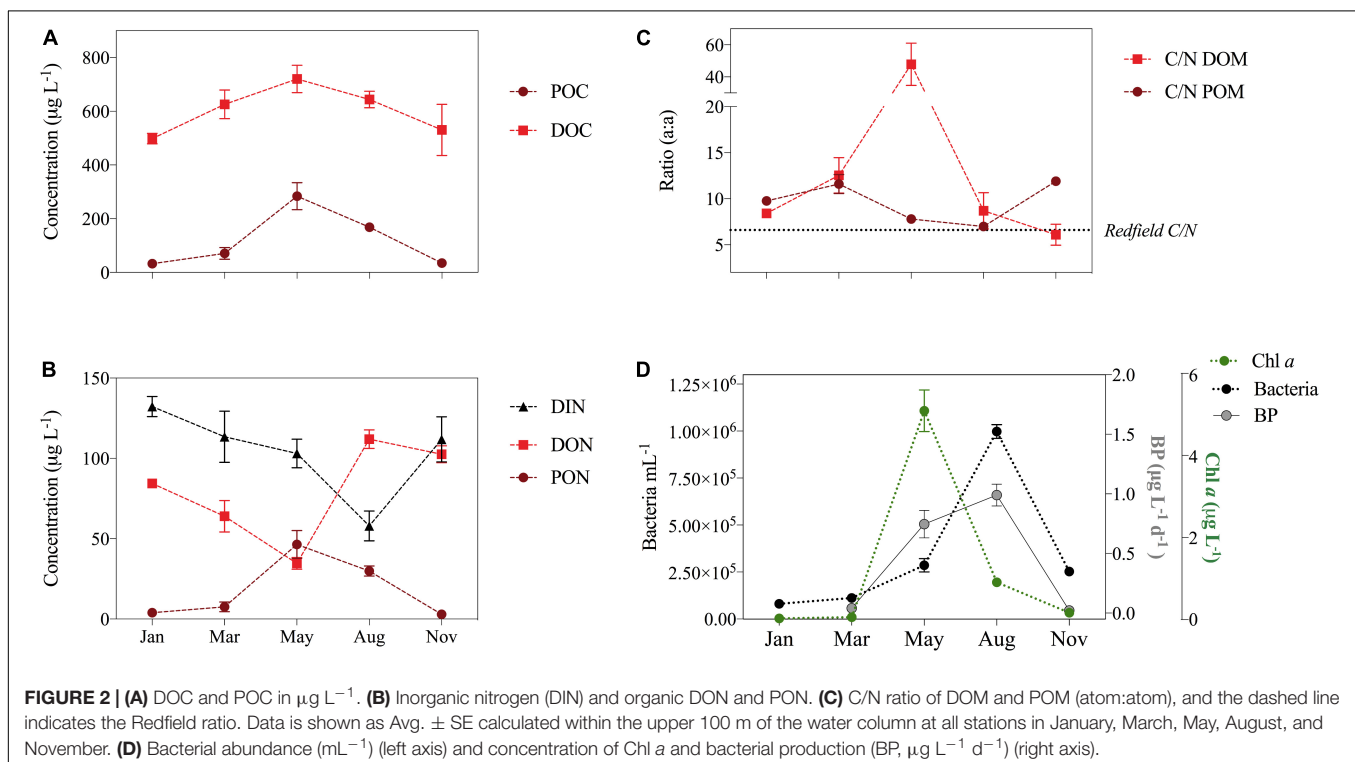
where $A(\lambda)$ is the absorbance at a given wavelength λ and l is the path length of a cuvette in meters (here 0.1 m). The spectral properties were modeled with an exponentially decreasing function and a constant using the software Prism 7.

$$a(\lambda) = a(\lambda_0)e^{-S(\lambda_0-\lambda)},$$

where S (nm^{-1}) is the spectral slope coefficient describing the relative steepness of the spectrum. The amplitude is a proxy for concentration, and the slope parameter is often used as a proxy for changes in the composition of CDOM (Stedmon and Markager, 2001; Twardowski et al., 2004). K is a background constant that allows for any baseline shifts or attenuation not caused by OM (Markager and Vincent, 2000). We here calculate the slope using most of the spectrum: $S[300\text{--}650 \text{ nm}]$ and within the UVB part of the spectrum only: $S[275\text{--}295 \text{ nm}]$.

Vertical Export of POM

Vertical export of POM within and out of the upper 200 m of the water column was measured by the deployment of a sediment trap array at all P-stations. The array was free drifting, either attached to an ice floe or hold by a buoy, and hence sampling was carried out in a semi-Lagrangian manner. The array had transparent plexiglass cylinders of 450 mm height and an inner diameter of 72 mm (aspect ratio 6.2) as traps, mounted to the array on a gimballed frame. No baffles were used in the cylinders opening, and no fixatives were added to the traps prior to deployment. Cylinders were deployed pairwise as traps at 20, 30, 40, 50, 60, 90, 120, and 200 m depth for 21 to 27 h. After recovery, the content in the traps was collected and subsamples processed for POC and PON, as described above. The traps used in this study (KC maskiner og laboratorieutstyr, Denmark) have been tested against ^{234}Th data from suspended and trapped material in the Barents Sea, demonstrating good catchment efficiency (Coppola et al., 2002).



Data Availability and Analyses

Data on microorganisms, Chl *a*, carbon and nitrogen measurements included in the paper are available from the data repository PANGAEA via Paulsen et al. (2017). Data were tested for normal distribution with a Shapiro–Wilk test in SPSS Statistics 23[®]. As normality was not given for all parameters, a non-parametric Spearman's correlation was applied to evaluate the covariation between different parameters.

RESULTS

To describe the production and fate of C and N pools the study included two different sampling strategies (1) measurements of C and N-pools along transects within the Atlantic inflow to the Arctic Ocean during five different seasons; winter (January), pre-bloom (March), spring bloom (May), post-bloom (August), early winter (November) (**Figure 1**) (2) dedicated process (P) stations focusing on the most productive season, May and August, to determine rates of PP and the sinking POM.

General Hydrography

All samples were collected within the Atlantic inflow to the Arctic Ocean and thus the dominating water masses were; the relatively warm and saline Atlantic Water (sal > 34.9, temp > 2°C) at the bottom and Arctic Surface Water at the surface, which is Atlantic water that has been influenced by sea ice melt and therefore is relatively colder and fresher (sal < 34.9). Sea ice samples from March indicate that sea ice meltwater is low in both DOC concentration ($480 \pm 80 \mu\text{g L}^{-1}$, $n = 4$) and CDOM absorption, e.g., $a_{\text{CDOM}}(290)$ ($0.28 \pm 0.04 \text{ m}^{-1}$, $n = 4$).

The Seasonal Cycle of Organic Matter

Throughout the year DOC dominated OM, with POC contributing successively more during the light season from March to May (**Figure 2A**). Both POC and PON displayed this seasonal pattern, with peak concentrations in May ($284 \pm 234 \mu\text{g POC L}^{-1}$, $46 \pm 41 \mu\text{g PON L}^{-1}$), causing a net accumulation of POM with a C/N ratio of 5.98 (calculated as $\Delta\text{POC}_{\text{January–May}}$ divided by $\Delta\text{PON}_{\text{January–May}}$) from January to May ($\Delta\text{POC}_{\text{January–May}}$ of $251 \mu\text{g POC L}^{-1}$ and $\Delta\text{PON}_{\text{January–May}}$ of $42 \mu\text{g N L}^{-1}$; **Table 1**). DOC concentrations also increased starting in January, peaking in May ($720 \pm 308 \mu\text{g DOC L}^{-1}$). The net accumulation of DOC from January to May ($\Delta\text{DOC}_{\text{January–May}} = 222 \mu\text{g C L}^{-1}$) was very similar to the net accumulation of POC during the same period.

Dissolved organic nitrogen concentrations, on the other hand, decreased from January to May, amounting to a net loss $\Delta\text{DON}_{\text{January–May}}$ of $49 \mu\text{g DON L}^{-1}$. DON concentrations then peaked in August ($109 \pm 36 \mu\text{g DON L}^{-1}$), corresponding to a $\Delta\text{DON}_{\text{May–August}}$ of $74 \mu\text{g DON L}^{-1}$ (**Table 1**). DIN decreased by $29 \mu\text{g DIN L}^{-1}$ from January to May meaning the DON-loss was 1.7 times larger than the DIN-loss. DIN continued to decrease until August (**Figure 2B** and **Table 1**), but not as much as DON. When summing the N-pools (PON, DON, and DIN) at the different seasons for the upper 100 m, the total nitrogen concentration (TN) remained stable throughout the period of

TABLE 1 | Average concentration (\pm SD; $\mu\text{g L}^{-1}$) of total, dissolved, and particulate organic carbon (TOC, DOC, and POC), as well as of dissolved, particulate organic nitrogen (DON, PON), and inorganic N (DIN) within the upper 100 m of the water column at all stations in January, March, May, August, and November.

	January		March		May		August		November	
	Avg \pm SD	Δ November–January	Avg \pm SD	Δ January–March	Avg \pm SD	Δ March–May	Avg \pm SD	Δ May–August	Avg \pm SD	Δ August–November
TOC	550 \pm 94 (80)	-260	661 \pm 129 (24)	111	964 \pm 299 (141)	303	805 \pm 180 (97)	-159	698 \pm 96 (16)	-124
DOC	498 \pm 90 (56)	-385	571 \pm 137 (13)	73	720 \pm 308 (86)	149	654 \pm 215 (95)	-66	647 \pm 99 (11)	-7
POC	33 \pm 9 (56)	-2	71 \pm 31 (13)	38	284 \pm 234 (86)	213	168 \pm 82 (103)	-116	35 \pm 6 (12)	-133
DON	84 \pm 9 (14)	3	51 \pm 32 (12)	-33	35 \pm 22 (64)	-16	109 \pm 36 (93)	74	81 \pm 10 (10)	-26
PON	4 \pm 1 (56)	1	8 \pm 5 (12)	3	46 \pm 41 (86)	38	30 \pm 17 (103)	-16	3 \pm 1 (11)	-27
DIN	132 \pm 27 (56)	21	113 \pm 34 (12)	-19	103 \pm 54 (86)	-10	58 \pm 55 (103)	-45	111 \pm 28 (11)	53
Δ POC: Δ PON				9.5		5.6		7.3		4.9

observations (averaging $201 \pm 15 \mu\text{g TN L}^{-1}$), with a maximum in January ($220 \pm 37 \mu\text{g TN L}^{-1}$) and a minimum in May ($184 \pm 116 \mu\text{g TN L}^{-1}$).

The different seasonal dynamics of organic C and N pools led to opposing seasonal patterns in the C/N ratio of POM and DOM (Figure 2C). Particulate C/N ratios exceeded 10 during the winter months of January, March, and November, while during the productive season they dropped to an average of 7.8 ± 1.6 and 7.0 ± 1.1 in May and August, respectively. For DOM, highest C/N ratios (on average 48 ± 79) were observed during the spring bloom in May, and lowest in January (on average 8.4 ± 0.5) and August (on average 8.7 ± 11.4).

The pattern of seasonal Chl *a* concentration mirrored the pattern of POM, with highest average concentrations in May (Figure 2A). Consequently, Chl *a* and POC were strongly positively correlated in the annual dataset (Table 2). Annual concentration of DOC also co-varied with Chl *a*, albeit not as strongly as POC and PON. DON correlated negatively with Chl *a*. The concentrations of POC, PON, and DON were correlated negatively with DIN, while no such correlation was found for DOC. The highest abundances of bacteria (Figure 2D) and HNF were observed in August (Supplementary Figures S2, S3), as were highest median bacterial production rates (Figure 2D). However, the cell specific bacterial production was highest in May. Bacterial abundances correlated positively to the concentration of DON and weakly negatively to DOC, while BP correlated negatively to DOC and unrelated to DON (Table 2).

Seasonal Change in CDOM

The absorption spectrum provides both quantitative and qualitative information about CDOM. The intensity of absorption, $a(\lambda)$, at a specific wavelength (λ) is used as an expression of the CDOM concentration. The shape of the absorption spectrum, which can be described by the slope (S) indicates changes in CDOM composition. The absorption spectra of surface water (1–100 m) were averaged for each month and showed seasonal changes in the character of DOM (Figure 3) with the distinct absorption peak within the UV spectrum around 290 nm (range: 260–310 nm) in May being the most prominent change (Figure 3A). Vertically $a_{\text{CDOM}}(290)$ was elevated around 30–40 m at P1 and 2 but was not elevated at P3 (Supplementary Figure S1), and the absorption peak was further present below 100 m (data not shown) in May. In August, the spring-peak signal had disappeared (Figure 3A and Supplementary Figure S1) whereas a high absorption within the visible spectrum (400–600 nm) appeared. In the winter months, absorption in the visible spectrum was generally lower than in August and May (Figures 3B,C). The shape of the absorption spectrum was examined by fitting the exponential model. The slope estimated for the small UVB wavelength range S [275–295 nm] was by far lowest in May, and slightly lower in January and March (29.3 – $29.9 \mu\text{m}^{-1}$) than in August and November (30.7 – $31.8 \mu\text{m}^{-1}$). The slope of full spectrum S [300–650 nm] increased gradually from January ($16.1 \mu\text{m}^{-1}$) to March ($20.3 \mu\text{m}^{-1}$) to May ($25.7 \mu\text{m}^{-1}$), after which it decreased to $19.2 \mu\text{m}^{-1}$ in August and $18.9 \mu\text{m}^{-1}$ in November. It should be

noted that given the shape of the absorption spectra in May, the fit was poor for this month, i.e., low R^2 values (Figures 3C,D).

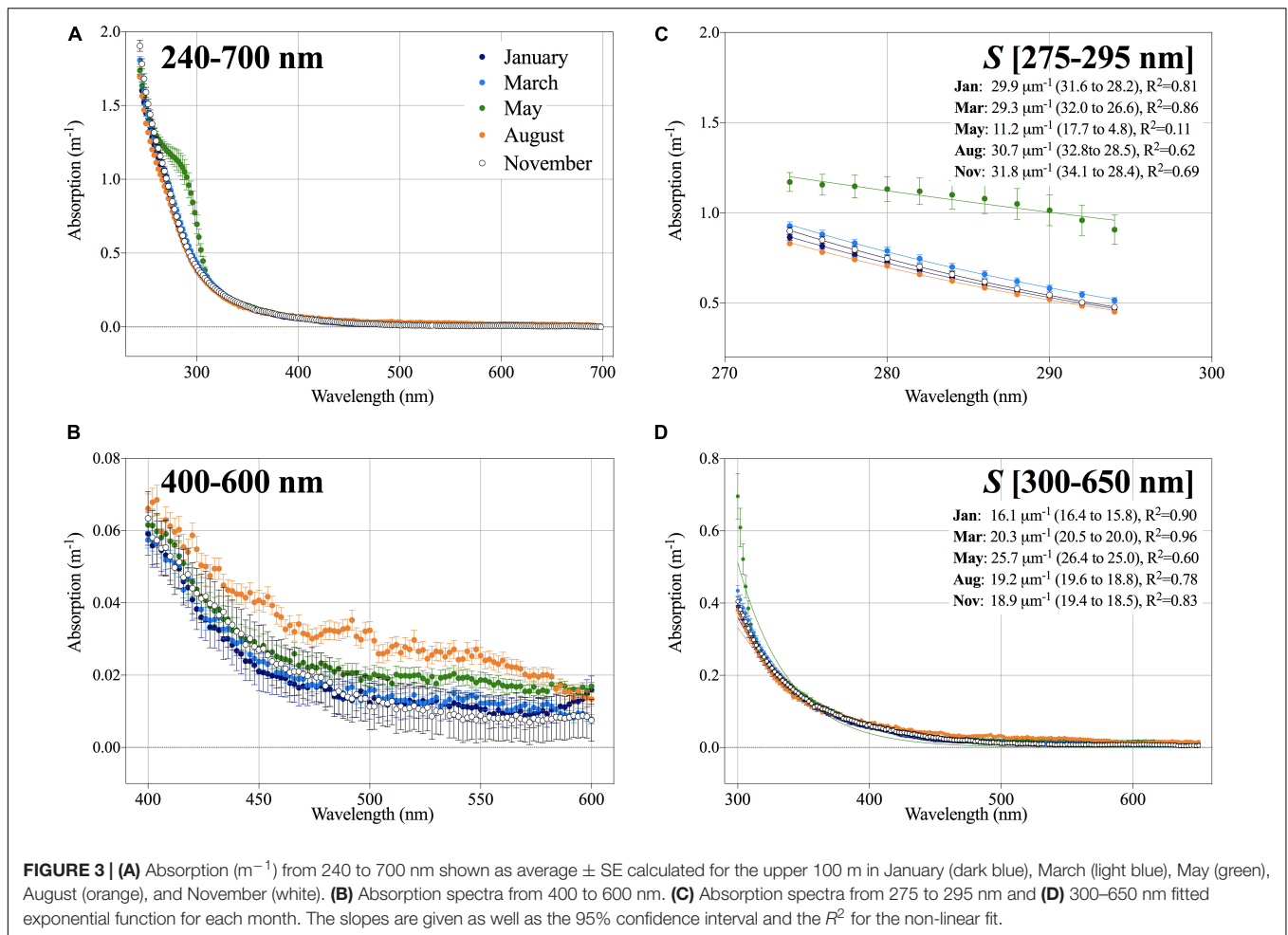
Physical Regime During Spring and Post-bloom

All process (P)-stations that were studied in more depth during the productive season were situated close to the ice edge Northwest-North of Svalbard (Figure 1). They shared similar hydrography, with Arctic Surface Water dominating the upper 40 m and Atlantic Water below. One exception was northernmost station P6, where Arctic Surface Water reached 150 m depth. The surface layer was fresher and warmer in August (Figures 4A,B) compared to May. The mixed layer depth was similar in May (10–11 m) and in August (9–15 m), while the photic zone deepened from approximately 20 m in May to 40 m in August (Figures 4A,B). For a more detailed description of the bloom stages and hydrography at the P-stations see Supplementary Table S1 and [Reigstad and Wassmann, 2007; Randelhoff et al., 2018 (current special issue)]. In the following paragraphs, we present an average of the three P-stations profiles examined during spring bloom and post-bloom are plotted, in order to better visualize the differences between the two seasons. Every single P-station profile is included as Supplementary Figures S1, S2.

Primary and Secondary Production During Spring and Post-bloom

In May, an intensive ice-edge bloom was encountered at all three P-stations sampled and strong vertical gradients in PP were observed at all three P-stations (Figures 4C–E). For both PP_{part} and PP_{diss} , higher production rates were measured within the sea ice meltwater-influenced upper 10 m of the water column than below the pycnocline ($<1 \mu\text{g C L}^{-1} \text{d}^{-1}$). Maximum surface rates ($\text{PP}_{\text{part}} = 250$ and $\text{PP}_{\text{diss}} = 345 \mu\text{g C L}^{-1} \text{d}^{-1}$) were observed at station P1 (Supplementary Figure S1). PP rates in August were more than five times lower than in May and peaked in subsurface waters (Figures 4C,D). Highest PP_{part} ($45 \mu\text{g C L}^{-1} \text{d}^{-1}$) was measured at 10 m of station P7. PP_{part} rates dropped to $<1 \mu\text{g C L}^{-1} \text{d}^{-1}$ below 40 m depth at all stations in August, and hence elevated PP_{part} rates reached deeper in August than in May. The vertical profile of PP_{diss} did not mimic that of PP_{part} in August (Figures 4C,D). The highest rate of PP_{diss} ($21 \mu\text{g C L}^{-1} \text{d}^{-1}$) was measured at 10 m of station P5, while PP_{diss} rates at station P6 and P7 did not exceed $4 \mu\text{g C L}^{-1} \text{d}^{-1}$ at any depths. The relationship between PP_{diss} and PP_{part} differed between May and August. In May, PP_{diss} was strongly correlated to PP_{part} and moderately correlated to both total Chl *a* and Chl *a* $> 10 \mu\text{m}$ (Table 3), whereas similar relationships were not observed in August. Further, a moderate negative correlation of PP_{diss} with the concentration of DIN was found in May, but not in August (Table 3). On average, % PP_{diss} was lower within the upper 20 m in August (19%) than in May (32%). % PP_{diss} varied between 3 to 98% in May and 2 to 77% in August and showed a clear increase with depth (Figure 4E).

Chl *a* in the upper 20 m was 10-fold higher in May than in August (Figure 4F), resulting in higher productivity specific



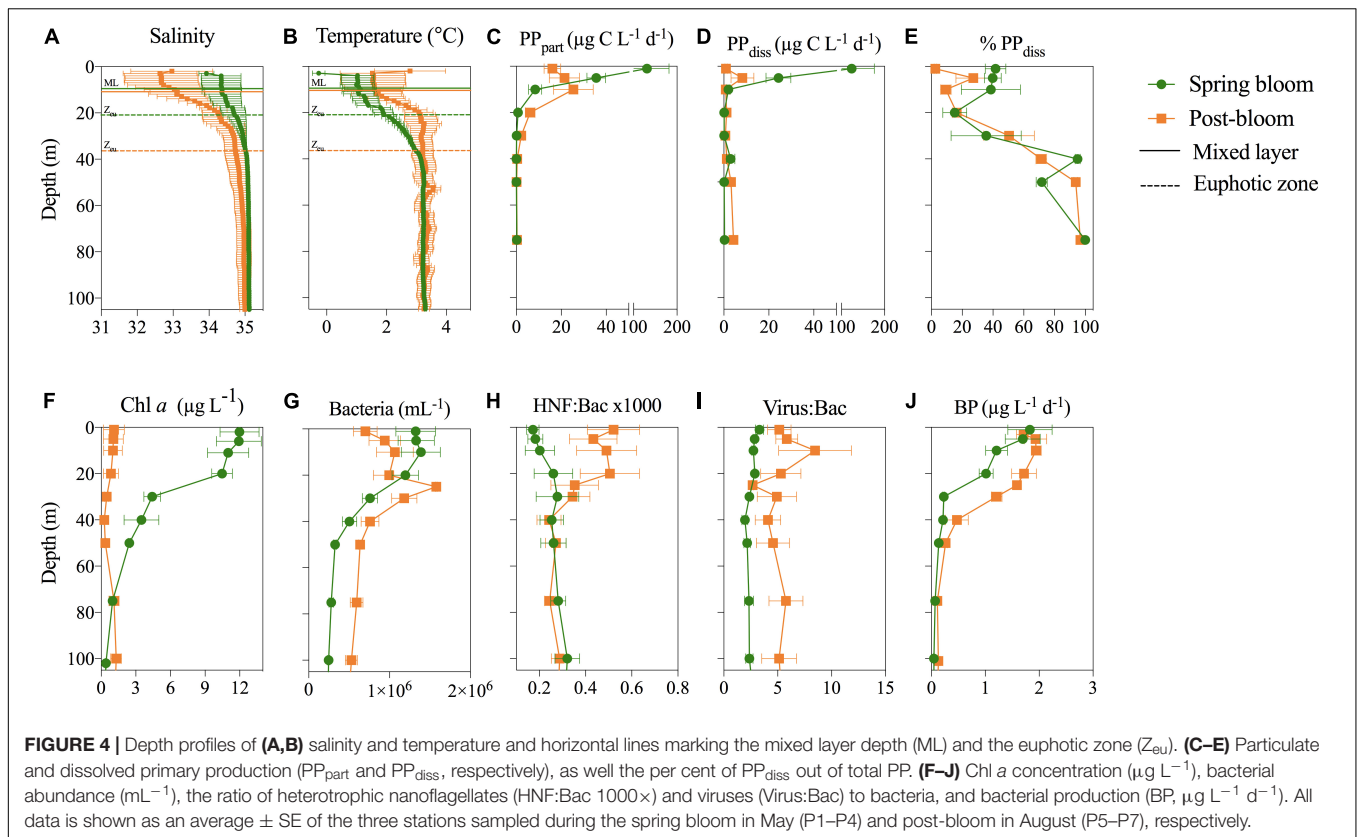
to phytoplankton biomass (based on Chl *a*) post-bloom. The abundance of bacteria, virus, and heterotrophic nanoflagellates (HNF) correlated positively with Chl *a* and PP_{part} in both

in May and August, but not to PP_{diss} (Table 3). The highest heterotrophic microbial abundances ($0.5\text{--}2 \times 10^6$ bacteria mL^{-1} and HNF 200–1000 HNF mL^{-1}) were found within the

TABLE 2 | Correlation matrix (non-parametric Spearman's rho, ρ) for particulate organic carbon (POC), particulate organic nitrogen (PON), dissolved organic carbon (DOC), dissolved organic nitrogen (DON), chlorophyll *a* (Chl *a*), concentration of nitrate, nitrite and ammonium (DIN), bacterial production (BP), and abundance (Bac), as well as abundance of heterotrophic nanoflagellates (HNF) and the abundance ratio of bacteria to virus (V:B) for the annual dataset.

		POC	PON	DOC	DON
Chl <i>a</i>	ρ	0.823**	0.819**	0.213**	-0.460**
	<i>n</i>	261	259	215	150
DIN	ρ	-0.702**	-0.694**	-0.052	-0.330**
	<i>n</i>	263	261	216	153
BP	ρ	0.813**	0.824**	-0.256**	-0.089
	<i>n</i>	105	104	86	71
Bac	ρ	0.302**	0.325**	-0.145*	0.402**
	<i>n</i>	240	238	192	152
HNF	ρ	0.581**	0.576**	-0.061	0.132
	<i>n</i>	240	238	192	152
V:B	ρ	-0.478**	-0.491**	-0.185**	0.265**
	<i>n</i>	240	238	192	152

**Correlation is significant at the 0.01 level *Correlation is significant at the 0.05 level.



productive upper 20 m of the water column at all P-stations. Bacterial abundance was slightly higher in the upper 20 m in May than August, while the subsurface abundances were highest in August (Figure 4G). Top-down control on bacteria is indicated by the ratio of HNF to bacteria (HNF:Bac $\times 1000$) and virus to bacteria (Virus:Bac), which are both elevated post-bloom relative to spring (Figures 4H,I). The ratio of HNF to bacteria averaged 0.3 ± 0.1 (3000 bacteria per HNF) below the pycnocline but increased to 0.5 ± 0.1 within the upper 20 m in August. Virus:Bac ratios averaged 1.9 ± 0.3 in the productive layer in May but increased to around 5 throughout the water column in August (Figure 4I).

Bacterial production (BP) rates were highest close to the surface ($3 \mu\text{g C L}^{-1} \text{d}^{-1}$) and dropped to $<1 \mu\text{g C L}^{-1} \text{d}^{-1}$ below 30 m (Figure 4J). BP rates were significantly higher during post-bloom than during spring bloom (Figure 4J and Supplementary Figure S2). Thus, both biomass specific PP and BP were higher during post-bloom, with higher rates sustained deeper in the water column (0–40 m) than in spring. BP and cell-specific bacterial production (BP/B), were moderately correlated to the concentration of Chl *a* and PP_{part} in both May and August (Table 3). Their relationship to PP_{diss} , however, changed with the season, being strongly positively correlated to PP_{diss} in May but not in August. In both May and August, calculated BCD largely exceeded PP_{diss} , except in the upper 5 m of three stations sampled in May, where BCD amounted to $<50\%$ of PP_{diss} , with lowest bacterial PP_{diss} consumption at station P1 (2–32%) and with $\sim 47\%$ highest at

station P4. The relationship between primary and secondary bacterial production (depth-integrated values 0–75 m) was heavily steered by the high production rates in the shallow upper mixed layer (Figure 5), indicating that depth-integrated PP_{diss} largely exceeded BCD at station P1 and P3, while BCD exceeded PP_{diss} at station P4 and all stations sampled in August.

Vertical Distribution of Organic Matter During Spring and Post-bloom

Dissolved organic carbon formed by far the largest carbon pool, with concentrations generally 10–30 times higher than POC, the only exception being within the shallow mixed surface layer in May, where DOC and POC were of the same order of magnitude. Maximum POC concentrations of 878 and $336 \mu\text{g L}^{-1}$ were found within the upper 20 m in May and August, respectively (Figure 6B). DOC concentrations did not display a pronounced vertical decrease similar to that of POC, with DOC concentration in the upper 100 m ($720 \pm 250 \mu\text{g L}^{-1}$) never significantly exceeding concentrations in the deep 750–1000 m samples ($695 \pm 76 \mu\text{g L}^{-1}$) even during the productive season. As a result, the DOC/POC ratio was <5 in the upper 30 m and 2–3 times higher at depth (Figure 6C). DOC concentrations did not vary significantly within the upper 100 m between May and August (Figure 6A and Table 1), in contrast to the clear shift observed in the organic N-pools; PON was the largest N-pool in the upper 20 m in spring, whereas DON increased threefold

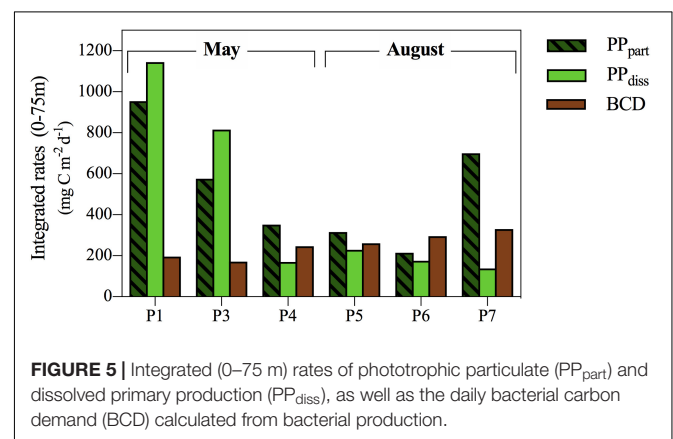
TABLE 3 | Correlation matrix (non-parametric Spearman's rho, ρ) of particulate primary production (PP_{part}), dissolved primary production (PP_{diss}), total chlorophyll *a* (Chl *a*), Chl *a* > 10 μm , concentration of nitrate, nitrite and ammonium (NO_x), bacterial abundance (Bac), bacterial production (BP) and cell-specific bacterial production (BP/B) in May and August.

			PP_{part}	PP_{diss}	Chl <i>a</i>	Chl <i>a</i> > 10 μm	NO_x
MAY	PP_{diss}	ρ	0.699**				
		<i>n</i>	19				
	Chl <i>a</i>	ρ	0.766**	0.495*			
		<i>n</i>	22	21			
	Chl > 10 μm	ρ	0.737**	0.465*	0.971**		
		<i>n</i>	22	21	24		
	NO_x	ρ	-0.799**	-0.593**	-0.705**	-0.703**	
		<i>n</i>	22	21	24	24	
	Bac	ρ	0.771**	0.431	0.723**	0.746**	-0.859**
		<i>n</i>	22	21	24	24	24
	BP	ρ	0.810**	0.619**	0.657**	0.681**	-0.848**
		<i>n</i>	22	21	24	24	24
	BP/Bac	ρ	0.666**	0.608**	0.458*	0.494*	-0.708**
		<i>n</i>	22	21	24	24	24
AUG.	PP_{diss}	ρ	0.108				
		<i>n</i>	17				
	Chl <i>a</i>	ρ	0.572**	0.164			
		<i>n</i>	23	17			
	Chl > 10 μm	ρ	0.495*	0.216	0.902**		
		<i>n</i>	23	17	26		
	NO_x	ρ	-0.694**	0.082	-0.434*	-0.253	
		<i>n</i>	21	15	22	22	
	Bac	ρ	0.678**	0.147	0.868**	0.933**	-0.378
		<i>n</i>	23	17	26	26	22
	BP	ρ	0.890**	0.015	0.736**	0.650**	-0.807**
		<i>n</i>	23	17	26	26	22
	BP/Bac	ρ	0.752**	-0.135	0.411*	0.249	-0.909**
		<i>n</i>	23	17	26	26	22

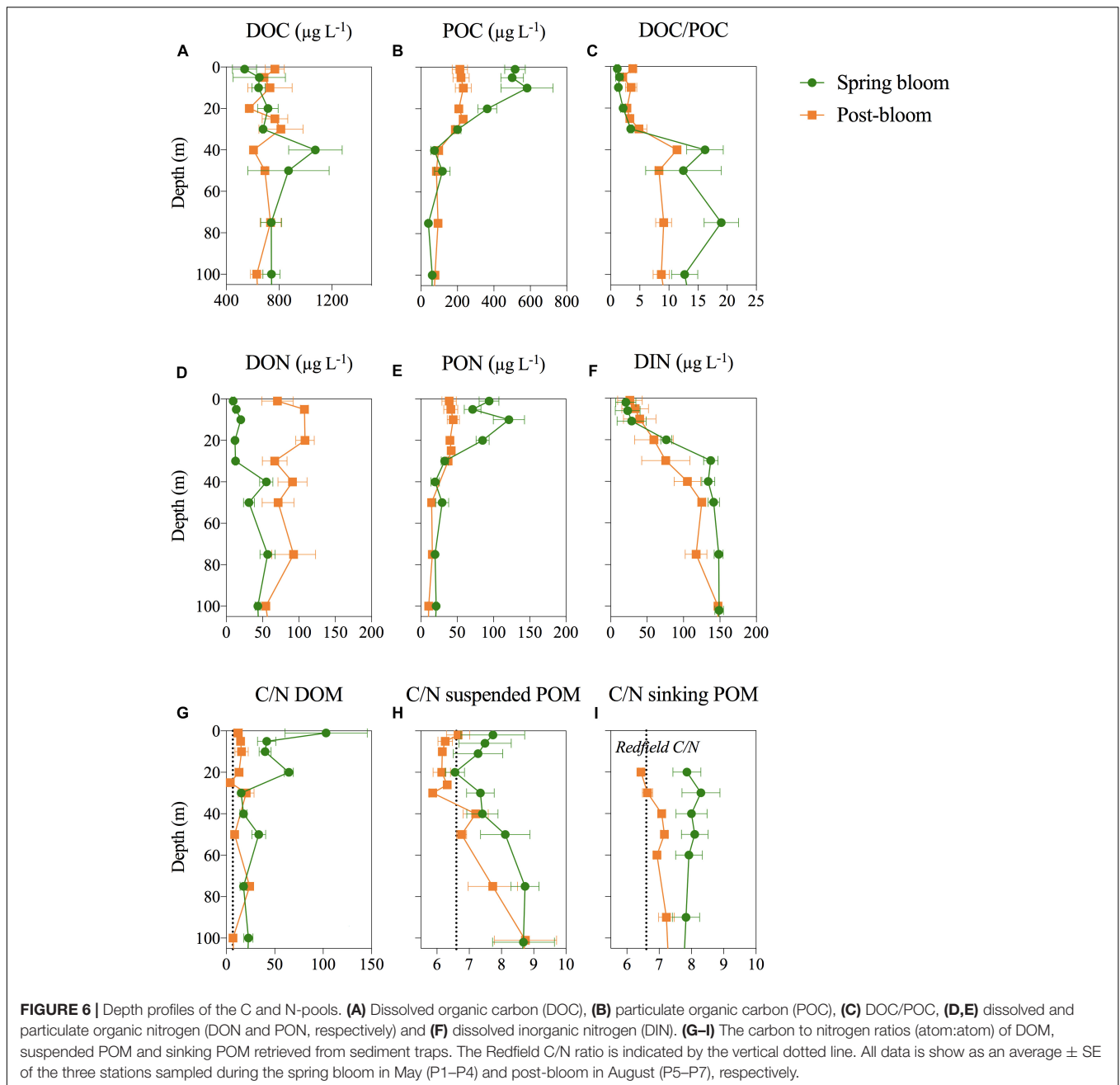
**Correlation is significant at the 0.01 level *Correlation is significant at the 0.05 level. Data from P-stations (0–75 m depth).

and was dominating the N-pool in August (Figures 6D,E and Table 1). The dissolved inorganic N (DIN) pool was equally low ($<2 \mu\text{g L}^{-1}$) in May and August in the upper 10 m but continued to decrease in subsurface waters (20–80 m) from May to August (Figure 6F). As a result, DON comprised the largest N pool within the productive surface layer during post-bloom. Both in May and August, POC was strongly positively correlated with Chl *a* and PP_{part} , and negatively correlated to DIN (Supplementary Table S2). For DOC, these correlations were weaker both on annual and monthly timescales. DOC and DON were weakly negatively correlated with Chl *a*, uncorrelated to both PP_{part} and PP_{diss} , and weakly positively correlated to DIN in May. In August, DOM was not significantly related to PP_{part} , PP_{diss} , Chl *a* nor DIN, except for a negative correlation between DON and DIN (Supplementary Table S2).

During the phytoplankton spring bloom in May, the C/N ratios of the DOM pool were high (avg. 43 ± 45 within the upper 100 m) with a maximum of 179 at 1 m at station P1 (Supplementary Figure S2). In August, the dissolved pool was characterized by low C/N ratios (average 10 ± 14 ; range: 4–99), when DON concentrations were high (Figure 6A). Suspended POM had C/N ratios close to Redfield in the upper 200 m

**FIGURE 5** | Integrated (0–75 m) rates of phototrophic particulate (PP_{part}) and dissolved primary production (PP_{diss}), as well as the daily bacterial carbon demand (BCD) calculated from bacterial production.

both May (7.7 ± 0.6) and slightly lower in August (6.9 ± 0.9), although elevated ratios ($\text{C/N} \geq 10$) were observed at station P4 (Supplementary Figure S2). We observed the lowest C/N of suspended POM at ca. 20 m and found an increase toward 100 m during both post- and spring bloom (Figure 6H). The C/N ratio of sinking POM reflected largely that of suspended POM



at the same station but showed less vertical variability than the suspended POM (Figure 6I).

DISCUSSION

Dissolved Primary Production and Other Sources of DOM

The PP changed notably from spring to post-bloom conditions (Figures 4, 5). The significant contribution of PP_{diss} to total PP in May and August are both higher than corresponding values from the Nordic Seas during summer [Poulton et al. (2016); avg. 15%,

range 2–46%], but within the range of previous measurements from the central Arctic Ocean Gosselin et al. (1997) and the Barents Sea (Vernet et al., 1998). A positive relationship between PP_{part} and PP_{diss} is expected when physiologically-driven extracellular release from vital phytoplankton is the dominating mechanism of DOM production (Baines and Pace, 1991), while the absence of such a relationship may be interpreted as trophic interactions being the primary release mechanism of DOM (Teira et al., 2003). The significant relationship between PP_{part} and PP_{diss} as observed in May, but not in August, thus suggests that physiological processes dominated DOM production under the spring bloom, while trophic interactions

became more important under post-bloom conditions. PP_{diss} correlated significantly and positively to $Chl\ a > 10\ \mu m$ (Table 3), presumably because diatoms and colonies of *P. pouchetii*, which dominated the phytoplankton community during the spring bloom and are known to release DOM during growth, were important producers of PP_{diss} (Ittekkot et al., 1981; Mykkestad, 1995; Alderkamp et al., 2007). In August, the solar irradiance was lower and phytoplankton biomass and production were reduced, while heterotrophic processes had increased bacterial production and the ratio of virus and HNF to bacteria had increased (Figure 4). The system had entered a stage of regenerated production (Randelhoff et al., 2016), with small phytoplankton and heterotrophic microorganisms dominating the plankton (Paulsen et al., 2016). Size-fractionation experiments further suggested a high degree of bacterivory and predation on picophytoplankton by heterotrophic flagellates (Paulsen et al., 2016). These observations support the notion that trophic interactions were important for DOM production (Taylor et al., 1985; Nagata and Kirchman, 1991) and responsible for the decorrelation of PP_{part} and PP_{diss} in August.

Phytoplankton Impact on the C/N Ratio of Organic Matter

Active DOM release by phytoplankton (the suggested May situation), has been described as an overflow mechanism by which phytoplankton releases excess photosynthate, ensuring a balance between carbon demand for anabolism and photosynthetic assimilation (Berman-Frank and Dubinsky, 1999). Freshly produced phytoplankton DOM is rich in carbon (Sambrotto et al., 1993; Søndergaard et al., 2000) and may explain the high C/N ratio in May (Figures 2A, 6G). Moreover, large-celled phytoplankton normally releases relatively less DON than smaller phytoplankton (Hasegawa et al., 2000; Varela et al., 2006), and the shift in phytoplankton size from diatoms and *Phaeocystis* in May to pico- and nano-sized autotrophs in August likely increased the release of DON relative to DOC during summer. In addition, trophic interactions led to the release of DOM with a C/N ratio closer to the Redfield ratio. Both mechanisms work in the direction of N-enriched DOM production in August, resulting in the observed seasonal difference in DON release. Randelhoff et al. (2016) report low *in situ* concentrations of nitrate within the euphotic zone in August, despite relative high upward turbulent diffusive nitrate flux across the nitracline, and low assimilation of nitrate into phytoplankton cells, which support our interpretation.

Potential Fate of POC and PON

The seasonal dynamics in the POM pool suggested that nitrogen incorporated in POM was rapidly sinking out of the upper 100 m of the water column during the productive season. C/N of accumulated POM was lowest during the productive period in May (7.8) and August (6.9), close to both Redfield ratio and averaged C/N ratios reported from the Arctic Ocean and pan-Arctic shelves (7.4; Frigstad et al., 2014). Almost identical C/N ratio of suspended and sinking POM in May and August indicate that the flux was too high for the system to degrade sinking POM within the surface and thus N is not retained in the surface waters

opposed to what Tamelander et al. (2013) suggest. The sinking loss of PON helps to close the annual N-budget, as it explains the drop in total N (TN) during the productive season. Other factors may affect the C/N ratio of sinking POM. Colonization of sinking particles by bacteria and other heterotrophic microbes (that were all more abundant during post-bloom), for example, could have increased the nitrogen content of initially nitrate-deprived sinking POM (Kawakami et al., 2007). Further, phytoplankton composition affects the stoichiometry of sinking material (Olli et al., 2002). Diatoms, for example, export relatively more carbon than *P. pouchetii*, most likely due to their large lipid reserves (Reigstad and Wassmann, 2007; Le Moigne et al., 2015). Indeed, diatoms were more abundant than *P. pouchetii* in May, where export C/N ratios were slightly higher than in August (Figure 6I and Supplementary Figure S2). Whatever the exact mechanisms behind the relatively larger net loss of PON from May to August, the data are coherent with earlier observations that diatoms and other large-celled phytoplankton are crucial for effective export of POC to depth (Lalande et al., 2013).

Bacterial Turnover of DOM

The net accumulation of DOM in the surface waters during spring (Figure 2A) suggests a decoupling between the biological production and consumption of DOM. DOC accumulating in the water column over the spring as well as the observed increase in the $a_{CDOM}(260-310)$ signal in March relative to the other winter months (Figure 3C), indicate that DOC production exceeded DOC loss rates as early as March. In this context it is worth noting that PP_{diss} largely exceeded estimated BCD at the stations where the phytoplankton spring bloom was still growing (station P1) or just had reached stationary growth (station P3) (Figure 5), indicating that bacteria were not able to use all of the newly produced DOC. As soon as the bloom started to decay (i.e., station P4), the estimated BCD slightly exceeded PP_{diss} , and a tighter coupling between the two was observed as the bloom progressed.

Bacterial carbon demand depends heavily on the growth efficiency (BGE) of the respective community (del Giorgio and Cole, 1998). BGE, in turn, depends on the taxonomic composition of the bacterial community (Reinthal and Herndl, 2005), temperature (Kritzberg et al., 2010), as well as the quality of DOM (del Giorgio and Cole, 1998; Wear et al., 2015). Most often BGE increases with bloom progression (Carlson and Hansell, 2013; Wear et al., 2015) and assuming this was the case in our study, the calculated BCD was overestimated for the early bloom (P1), and underestimated for the decaying bloom (P4). This only strengthens our hypothesis of tighter coupling between PP_{diss} and BCD as the bloom progressed, which is furthermore supported by the significant positive correlation between PP_{diss} and BP in May. The question remains though why the bacterial community, although stimulated by PP_{diss} , were not able to consume DOM at the same rate as it was produced. Limitation of bacterial production by inorganic nutrients (Zweifel et al., 1993; Thingstad et al., 1997), low bioavailability of the DOC (Carlson et al., 1996), inhibition of bacterial growth by low temperatures (Pomeroy and Deibel, 1986), and high bacterial mortality due to high grazing pressure (Zweifel, 1999; Duarte

et al., 2005), are all mechanisms proposed to explain why DOC escapes bacterial degradation and accumulates above background levels in the ocean's surface. In our case, limitation by inorganic nutrients appears unlikely, as DOC started to accumulate early in the season when nutrients were still ample. The organisms dominating the spring bloom phytoplankton community, diatoms and *Phaeocystis*, are known to release complex DOM compounds, which might be less bio-available to bacteria (Aluwihare and Repeta, 1999; Alderkamp et al., 2007). However, bacterial groups known to be effective consumers of diatom exudates proliferated at the P-stations in May (Wilson et al., 2017) and should have been able to utilize freshly produced DOC. The high absorption signal within the UV region $a_{\text{CDOM}}(260\text{--}300)$ produced during spring bloom and possibly transformed to an absorption signal within the visible spectra by August indeed indicate that bacteria might have partly mediated the transformation of fresh and labile DOC into more degradation-resistant molecules, as suggested by Lechtenfeld et al. (2015).

Surprisingly, the release and uptake of DON were seasonally out of phase with that of DOC. While DOC was at its lowest during winter, DON decreased during spring and was at a minimum in May. A possible explanation is that when DIN becomes limiting, the demand for organically bound N increases. Extensive DON uptake and remineralization by heterotrophs during early bloom development has been suggested previously by experimental and modeling work (Van den Meersche et al., 2004). However, phytoplankton may also obtain a substantial part of their N via DON (Bronk et al., 2007). Further studies are needed to identify which organisms are responsible for the POM production by uptake of DON during late winter-early spring. Whatever the reasons underlying the mobilization of the DON pool in spring, our data suggest that the significant spring accumulation of POM was not only based on inorganic nitrogen sources, but also on organic ones.

Seasonal Changes in the Characteristics of CDOM

The CDOM absorption spectra agree with previous observations in the Fram Strait region (Pavlov et al., 2015). The relatively low values reflect that the study was conducted within Atlantic influenced water, as Atlantic water carries low amount of both CDOM and fluorescent DOM relative to the Arctic water (Jørgensen et al., 2014; Pavlov et al., 2015). Also, the $S[300\text{--}650\text{ nm}]$ estimated here (range: 16–26) are similar to those found within Atlantic water in Fram Strait region (Granskog et al., 2012) (range 14–32).

Colored dissolved organic matter absorption has never previously been measured during a full annual cycle in this region and the absorption peak within the UV spectrum $a_{\text{CDOM}}(260\text{--}310\text{ nm})$ in May (Figure 3A) not previously described. The $a_{\text{CDOM}}(260\text{--}310)$ does not correlate directly with Chl *a* or PP, and photosynthates are not be expected to absorb light. Rather, this peak could be indirectly linked to the spring bloom production, similar to what was observed in a Svalbard mesocosm experiment, where high CDOM absorption within the UV band [$a_{\text{CDOM}}(310\text{--}360\text{ nm})$] was attributed to increased

bacterial activity following maximum PP (Pavlov et al., 2014). The signal could alternatively be related to mycosporine-like amino acids (MAAs), secondary phytoplankton metabolites that also produce an absorption maxima within the UV band (Vernet and Whitehead, 1996). These were previously reported at high concentrations in a *Phaeocystis* sp. dominated Svalbard fjord, even when Chl *a* concentrations were low (Ha et al., 2012).

There is generally a negative correlation between $S[500\text{--}700\text{ nm}]$ and molecular weight of DOM, while slope values for the UVB wavelength range $S[275\text{--}295\text{ nm}]$ are correlated with positively molecular weight (Stedmon and Nelson, 2015). As the slope value for May is low in the UVB range and high in the visible range, this suggest that DOM in May had lower molecular weight than DOM in the other months. This agrees with the observed high PP_{diss} in May and the accumulation of small carbon-rich molecules, with the 'early bloom-stage' P1 having both the highest PP_{diss} and the highest $a_{\text{CDOM}}(290)$ (Supplementary Figure S1). Our CDOM observations further indicate that the spring bloom OM is transformed as soon as August and thus that OM produced during summer at the ice edge is altered before reaching the central Arctic Ocean.

Arctic Perspective and Significance

The present study demonstrates that the strongly seasonal pulsed production in the marginal ice zone allows for a temporal decoupling of the production and the utilization of OM, and hence the accumulation of both POM and DOM above background concentrations in surface waters in spring and summer. The results caution against calculations of PP_{part} from winter nitrate drawdown (as is done in several studies i.e., Tremblay et al., 2006; Randelhoff et al., 2015). Almost half of the accumulated organic carbon from January to May was found as DOM, and hence POM production estimated from nitrate drawdown would lead to a severe overestimation of POM available for trophic transfer or potential export to depth. Our results are in agreement with earlier studies suggesting DON play an essential role in the N-cycle of sea ice influenced waters in Arctic systems (Skoog et al., 2001; Davis and Benner, 2005; Mei et al., 2005) and thus further cautions calculations of PP_{part} from winter nitrate drawdown, as DON apparently is an active N-source. The large DON pool that accumulated during post-bloom could serve as important nitrogen storage in stratified DIN-depleted waters and serve as a substrate for microbial production well beyond the productive season. We, therefore, recommend organic N-pools are investigated when studying biogeochemical cycling in the Arctic Ocean. Our findings also encourage future studies to identify which organisms are responsible for the uptake of DON in late winter-early spring and how this influence the entire POM production in relation to the DIN budget.

AUTHOR CONTRIBUTIONS

LS and MP equally lead the data analysis and the writing of the article. LS performed measurements of bacterial production and POM. MP was responsible for bacterial counts, DOM

and CDOM measurements. MV and MC were in charge of primary production measurements. All authors contributed to the interpretation of the data and commented on the text.

FUNDING

This work was conducted within the framework of the research projects CarbonBridge (RCN 226415) and MicroPolar (RCN 225956), both funded by the Norwegian Research Council.

ACKNOWLEDGMENTS

We wish to thank the crews of RV Helmer Hanssen and RV Lance for their great logistical support during the cruises. A special thanks to Jean-Eric Tremblay and Svein Kristiansen for providing data on inorganic nutrients, as well as Achim Randelhoff for providing information on water column stability.

SUPPLEMENTARY MATERIAL

The Supplementary Material for this article can be found online at: <https://www.frontiersin.org/articles/10.3389/fmars.2018.00416/full#supplementary-material>

FIGURE S1 | Depth profiles of particulate and dissolved primary production (PP_{part} and PP_{diss} , respectively), and the percent of PP_{diss} , as well as the

absorption of CDOM at 290 nm, bacterial production and the bacterial carbon demand as percent of dissolved primary production (PP_{diss}) for the stations in May (**upper**; P1–P4) and August (**lower**; P5–P7). 100% is indicated by a dashed line.

FIGURE S2 | Depth profiles of carbon to nitrogen ratios (atom : atom) of dissolved organic matter (DOM), particulate organic matter (POM), and sinking POM retrieved from sediment traps (dashed line indicates the Redfield ratio), and the abundance of bacteria and heterotrophic nanoflagellates as well as the ratio of virus to bacteria at all stations in May (**upper**) and August (**lower**). The P-stations are emphasized with circles in May and diamonds in August, while the gray lines indicate other stations sampled during the same month (**Figure 1**).

FIGURE S3 | Median and percentiles (5 and 95%) of abundance of heterotrophic nanoflagellates (HNF), the ratio of virus to bacteria (Virus:Bac), as well as bacterial production (BP) and cell-specific bacterial production (BP/Bac), within the upper 100 m of the water column at all stations in January, March, May, August, and November. Note difference in scales. No data (n.d.).

TABLE S1 | Overview over the conditions at the process station in May and August as given in Randelhoff et al. (2018): sea ice concentrations, depths of the mixed layer (d_{ML}), photic zone (Z_{ph}) and the upper and lower end of the nitracline (d_N) at each station. The water layer from the surface to the lower end of d_N defines here the productive layer (0–30 m in May; 0–40 m in August). The average concentration of nitrate and nitrite (NO_x), phosphate (PO_4^{3-}), silicate (Si), and chlorophyll *a* (Chl *a*) within the productive layer are given (range of concentrations given in brackets). The phytoplankton bloom stage is classified as given in Reigstad et al. (unpublished).

TABLE S2 | Correlation matrix (non-parametric Spearman's rho, ρ) of particulate organic carbon (POC), particulate organic nitrogen (PON), dissolved organic carbon (DOC), dissolved organic nitrogen (DON), nitrate, nitrite and ammonium (DIN), and chlorophyll *a* (Chl *a*) concentration at all depth (0–1000 m) at all stations in May and August.

REFERENCES

- Agusti, S., and Duarte, C. M. (2013). Phytoplankton lysis predicts dissolved organic carbon release in marine plankton communities. *Biogeosciences* 10, 1259–1264. doi: 10.5194/bg-10-1259-2013
- Alderkamp, A. C., Buma, A. G. J., and van Rijssel, M. (2007). The carbohydrates of *Phaeocystis* and their degradation in the microbial food web. *Biogeochemistry* 83, 99–118. doi: 10.1007/s10533-007-9078-2
- Aluwihare, L. I., and Repeta, D. J. (1999). A comparison of the chemical characteristics of oceanic DOM and extracellular DOM produced by marine algae. *Mar. Ecol. Prog. Ser.* 186, 105–117. doi: 10.3354/meps186105
- Assmy, P., Fernández-Méndez, M., Duarte, P., Meyer, A., Randelhoff, A., Mundy, C. J., et al. (2017). Leads in Arctic pack ice enable early phytoplankton blooms below snow-covered sea ice. *Sci. Rep.* 7:40850. doi: 10.1038/srep40850
- Baines, S. B., and Pace, M. L. (1991). The production of dissolved organic matter by phytoplankton and its importance to bacteria: patterns across marine and freshwater systems. *Limnol. Oceanogr.* 36, 1078–1090. doi: 10.4319/lo.1991.36.6.1078
- Bates, N. R., Hansell, D. A., Bradley Moran, S., and Codispoti, L. A. (2005). Seasonal and spatial distribution of particulate organic matter (POM) in the Chukchi and Beaufort Seas. *Deep Sea Res. Part II Top. Stud. Oceanogr.* 52, 3324–3343. doi: 10.1016/j.dsr2.2005.10.003
- Berman-Frank, I., and Dubinsky, Z. (1999). Balanced growth in aquatic plants: myth or reality? Phytoplankton use the imbalance between carbon assimilation and biomass production to their strategic advantage. *Bioscience* 49, 29–37. doi: 10.2307/1313491
- Bjornsen, P. K. (1988). Phytoplankton exudation of organic matter: why do healthy vells do it? *Limnol. Oceanogr.* 33, 151–154. doi: 10.4319/lo.1988.33.1.0151
- Bratbak, G., Heldal, M., Thingstad, T. F., Riemann, B., and Haslund, O. H. (1992). Incorporation of viruses into the budget of microbial C-transfer. A first approach. *Mar. Ecol. Prog. Ser.* 83, 273–280. doi: 10.3354/meps083273
- Bronk, D. A., Glibert, P. M., Malone, T. C., Banahan, S., and Sahlsten, E. (1998). Inorganic and organic nitrogen cycling in Chesapeake Bay: autotrophic versus heterotrophic processes and relationships to carbon flux. *Aquat. Microb. Ecol.* 15, 177–189. doi: 10.3354/ame015177
- Bronk, D. A., See, J. H., Bradley, P., and Killberg, L. (2007). DON as a source of bioavailable nitrogen for phytoplankton. *Biogeosciences* 4, 283–296. doi: 10.5194/bg-4-283-2007
- Carlson, C. A., Ducklow, H. W., and Sleeter, T. D. (1996). Stocks and dynamics of bacterioplankton in the northwestern Sargasso Sea. *Deep Sea Res. Part II Top. Stud. Oceanogr.* 43, 491–515. doi: 10.1016/0967-0645(95)00101-8
- Carlson, C. A., and Hansell, D. A. (2013). “The contribution of dissolved organic carbon and nitrogen to the biogeochemistry of the Ross Sea,” in *Biogeochemistry of the Ross Sea*, eds G. R. Ditullio and R. B. Dunbar (Washington, DC: American Geophysical Union), 123–142.
- Codispoti, L. A., Kelly, V., Thessen, A., Matrai, P., Suttles, S., Hill, V., et al. (2013). Synthesis of primary production in the Arctic Ocean: III. Nitrate and phosphate based estimates of net community production. *Prog. Oceanogr.* 110, 126–150. doi: 10.1016/j.pocean.2012.11.006
- Coppola, L., Roy-Barman, M., Wassmann, P., Mulsow, S., and Jeandel, C. (2002). Calibration of sediment traps and particulate organic carbon export using ^{234}Th in the Barents Sea. *Mar. Chem.* 80, 11–26. doi: 10.1016/S0304-4202(02)00071-3
- Davis, J., and Benner, R. (2005). Seasonal trends in the abundance, composition and bioavailability of particulate and dissolved organic matter in the Chukchi/Beaufort Seas and western Canada Basin. *Deep Sea Res. Part I Top. Stud. Oceanogr.* 52, 3396–3410. doi: 10.1016/j.dsr2.2005.09.006
- del Giorgio, P. A., and Cole, J. J. (1998). Bacterial growth efficiency in natural aquatic systems. *Annu. Rev. Ecol. Syst.* 29, 503–541. doi: 10.1146/annurev.ecolsys.29.1.503
- Dittmar, T., and Kattner, G. (2003). The biogeochemistry of the river and shelf ecosystem of the Arctic Ocean: a review. *Mar. Chem.* 83, 103–120. doi: 10.1016/S0304-4203(03)00105-1
- Duarte, C. M., Agusti, S., Vaqué, D., Agawin, N. S. R., Felipe, J., Casamayor, E. O., et al. (2005). Experimental test of bacteria-phytoplankton coupling in the

- Southern Ocean. *Limnol. Oceanogr.* 50, 1844–1854. doi: 10.4319/lo.2005.50.6.1844
- Ducklow, H. (2003). “Seasonal production and bacterial utilization of DOC in the Ross Sea, Antarctica,” in *Biochemistry of the Ross Sea*, eds G. DiTullio and R. Dunbar (Washington, DC: American Geophysical Union), 143–158.
- Engel, A., Piontek, J., Metfies, K., Endres, S., Sprong, P., Peeken, I., et al. (2017). Inter-annual variability of transparent exopolymer particles in the Arctic Ocean reveals high sensitivity to ecosystem changes. *Sci. Rep.* 7:4129. doi: 10.1038/s41598-017-04106-9
- Fahrbach, E., Meincke, J., Østerhus, S., Rohardt, G., Schauer, U., Tverberg, V., et al. (2001). Direct measurements of volume transports through Fram Strait. *Polar Res.* 20, 217–224. doi: 10.1111/j.1751-8369.2001.tb00059.x
- Fogg, G. E. (1983). The ecological significance of extracellular products of phytoplankton photosynthesis. *Bot. Mar.* 26, 3–14. doi: 10.1515/botm.1983.26.1.3
- Fransson, A., Chierici, M., Anderson, L. C., Bussmann, I., Kattner, G., Jones, E. P., et al. (2001). The importance of shelf processes for the modification of chemical constituents in the waters of the Eurasian Arctic Ocean: implication for carbon fluxes. *Cont. Shelf Res.* 21, 225–242. doi: 10.1016/s0278-4343(00)00088-1
- Frigstad, H., Andersen, T., Bellerby, R. G. J., Silyakova, A., and Hessen, D. O. (2014). Variation in the seston C:N ratio of the Arctic Ocean and pan-Arctic shelves. *J. Mar. Syst.* 129, 214–223. doi: 10.1016/j.jmarsys.2013.06.004
- Goldman, J. C., Caron, D. A., and Dennett, M. R. (1987). Regulation of gross growth efficiency and ammonium regeneration in bacteria by substrate C: N ratio. *Limnol. Oceanogr.* 32, 1239–1252. doi: 10.4319/lo.1987.32.6.1239
- Gosselin, M., Levasseur, M., Wheeler, P. A., Horner, R., and Booths, B. C. (1997). New measurements of phytoplankton and ice algal production in the Arctic Ocean. *Deep Sea Res. Part II Top. Stud. Oceanogr.* 44, 1623–1644. doi: 10.1016/S0967-0645(97)00054-4
- Granskog, M. A., Stedmon, C. A., Dodd, P. A., Amon, R. M. W., Pavlov, A. K., De Stur, L., et al. (2012). Characteristics of colored dissolved organic matter (CDOM) in the Arctic outflow in the Fram Strait: assessing the changes and fate of terrigenous CDOM in the Arctic Ocean. *J. Geophys. Res.* 117, 1–13. doi: 10.1029/2012JC008075
- Ha, S.-Y., Kim, Y.-N., Park, M.-O., Kang, S.-H., Kim, H., and Shin, K.-H. (2012). Production of mycosporine-like amino acids of in situ phytoplankton community in Kongsfjorden, Svalbard, Arctic. *J. Photochem. Photobiol. B Biol.* 114, 1–14. doi: 10.1016/j.jphotobiol.2012.03.011
- Hasegawa, T., Koike, I., and Mukai, H. (2000). Release of dissolved organic nitrogen by size-fractionated natural planktonic assemblages in coastal waters. *Mar. Ecol. Prog. Ser.* 198, 43–49. doi: 10.3354/meps198043
- Holding, J. M., Duarte, C. M., Mesa, E., Arrieta, J. M., Chierici, M., Hendriks, I. E., et al. (2015). Temperature dependence of CO₂-enhanced primary production in the European Arctic Ocean. *Nat. Clim. Chang.* 5, 1079–1082. doi: 10.1038/NCLIMATE2768
- Holmes, R. M., Aminot, A., K rouel, R., Hooker, B. A., and Peterson, B. J. (1999). A simple and precise method for measuring ammonium in marine and freshwater ecosystems. *Can. J. Fish. Aquat. Sci.* 56, 1801–1808. doi: 10.1139/f99-9-128
- Hopkinson, C. S., and Vallino, J. J. (2005). Efficient export of carbon to the deep ocean through dissolved organic matter. *Nature* 433, 142–145. doi: 10.1038/nature03191
- Ittekkot, V., Brockmann, U., Michaelis, W., and Degens, E. T. (1981). Dissolved free and combined carbohydrates during a phytoplankton bloom in the northern North Sea. *Mar. Ecol. Prog. Ser.* 4, 299–305. doi: 10.3354/meps004299
- J rgensen, L., Stedmon, C. A., Granskog, M. A., and Middelboe, M. (2014). Tracing the long-term microbial production of recalcitrant fluorescent dissolved organic matter. *Geophys. Res. Lett.* 41, 2481–2488. doi: 10.1002/2014GL059428
- Jumars, P. A., Penry, D. L., Baross, J. A., Perry, M. J., and Frost, B. W. (1989). Closing the microbial loop: dissolved carbon pathway to heterotrophic bacteria from incomplete ingestion, digestion and absorption in animals. *Deep Sea Res. Part A Oceanogr. Res. Papers* 36, 483–495. doi: 10.1016/0198-0149(89)90001-0
- Kawakami, H., Honda, M. C., Wakita, M., and Watanabe, S. (2007). Time-series observation of dissolved inorganic carbon and nutrients in the northwestern north pacific. *J. Oceanogr.* 63, 967–982. doi: 10.1007/s10872-007-0081-y
- Kirchman, D. (2001). Measuring bacterial biomass production and growth rates from leucine incorporation in natural aquatic environments. *Methods Microbiol.* 30, 227–237. doi: 10.1016/s0580-9517(01)30047-8
- Kirchman, D. L., Suzuki, Y., Garside, C., and Ducklow, H. W. (1991). High turnover rates of dissolved organic carbon during a spring phytoplankton bloom. *Nature* 352, 612–614. doi: 10.1038/352612a0
- Kivim ae, C., Bellerby, R. G. J., Fransson, A., Reigstad, M., and Johannessen, T. (2010). A carbon budget for the Barents Sea. *Deep Sea Res. Part I Oceanogr. Res. Papers* 57, 1532–1542. doi: 10.1016/j.dsr.2010.05.006
- Kritzberg, E. S., Duarte, C. M., and Wassmann, P. (2010). Changes in Arctic marine bacterial carbon metabolism in response to increasing temperature. *Polar Biol.* 33, 1673–1682. doi: 10.1007/s00300-010-0799-7
- Lalande, C., Bauerfeind, E., Nothig, E. M., and Beszczynska-Moller, A. (2013). Impact of a warm anomaly on export fluxes of biogenic matter in the eastern Fram Strait. *Prog. Oceanogr.* 109, 70–77. doi: 10.1016/j.pocean.2012.09.006
- Le Moigne, F. A. C., Poulton, A. J., Henson, S. A., Daniels, C. J., Fragoso, G. M., Mitchell, E., et al. (2015). Carbon export efficiency and phytoplankton community composition in the Atlantic sector of the Arctic Ocean. *J. Geophys. Res.* 120, 3896–3912. doi: 10.1002/2015jc010700
- Lechtenfeld, O. J., Hertkorn, N., Shen, Y., Witt, M., and Benner, R. (2015). Marine sequestration of carbon in bacterial metabolites. *Nat. Commun.* 6:6711. doi: 10.1038/ncomms7711
- Maranon, E., Cermeno, P., Fernandez, E., Rodriguez, J., and Zabala, L. (2004). Significance and mechanisms of photosynthetic production of dissolved organic carbon in a coastal eutrophic ecosystem. *Limnol. Oceanogr.* 49, 1652–1666. doi: 10.4319/lo.2004.49.5.1652
- Markager, S., and Vincent, W. (2000). Spectral light attenuation and the Absorption of UV and blue light in natural waters. *Limnol. Oceanogr.* 45, 642–650. doi: 10.4319/lo.2000.45.3.0642
- Mathis, J. T., Hansell, D. A., Kadko, D., Bates, N. R., and Cooper, L. W. (2007). Determining net dissolved organic carbon production in the hydrographically complex western Arctic Ocean. *Limnol. Oceanogr.* 52, 1789–1799. doi: 10.4319/lo.2007.52.5.1789
- Mei, Z. P., Legendre, L., Tremblay, J. E., Miller, L. A., Gratton, Y., Lovejoy, C., et al. (2005). Carbon to nitrogen (C: N) stoichiometry of the spring-summer phytoplankton bloom in the North Water Polynya (NOW). *Deep Sea Res. Part I Oceanogr. Res. Papers* 52, 2301–2314. doi: 10.1016/j.dsr.2005.07.001
- Middelboe, M., J rgensen, N. O. G., and Kroer, N. (1996). Effects of viruses on nutrient turnover and growth efficiency of noninfected marine bacterioplankton. *Appl. Environ. Microbiol.* 62, 1991–1997.
- Mykkestad, S., Holmhansen, O., Varum, K. M., and Volcani, B. E. (1989). Rate of release of extracellular amino acids and carbohydrates from the marine diatom *Chaetoceros affinis*. *J. Plankton Res.* 11, 763–773. doi: 10.1093/plankt/11.4.763
- Mykkestad, S. M. (1995). Release of extracellular products by phytoplankton with special emphasis on polysaccharides. *Sci. Total Environ.* 165, 155–164. doi: 10.1016/0048-9697(95)04549-g
- Nagata, T., and Kirchman, D. L. (1991). Release of dissolved free and combined amino-acids by bacterivorous marine flagellates. *Limnol. Oceanogr.* 36, 433–443. doi: 10.4319/lo.1991.36.3.0433
- Olli, K., Wexels Riser, C., Wassmann, P., Ratkova, T. N., Arashkevich, E., and Pasternak, A. (2002). Seasonal variation in vertical flux of biogenic matter in the marginal ice zone and the central Barents Sea. *J. Mar. Syst.* 38, 189–204. doi: 10.1016/S0924-7963(02)00177-X
- Paulsen, M. L., Bratbak, G., Larsen, A., Seuthe, L., Egge, J., and Erga, S. R. (2017). CarbonBridge 2014: physical oceanography and microorganism composition during 5 cruises (Jan, March, May, August, Nov 2014) on and off the shelf northwest of Svalbard in 2014. *Pangaea* doi: 10.1594/PANGAEA.884255
- Paulsen, M. L., Dor e, H., Garczarek, G., Seuthe, L., M ller, O., Sandaa, R.-A., et al. (2016). *Synechococcus* in the Atlantic Gateway to the Arctic Ocean. *Front. Mar. Sci.* 3:191. doi: 10.3389/fmars.2016.00191
- Pavlov, A. K., Granskog, M. A., Stedmon, C. A., Ivanov, B. V., Hudson, S. R., and Falk-petersen, S. (2015). Contrasting optical properties of surface waters across the Fram Strait and its potential biological implications. *J. Mar. Syst.* 143, 62–72. doi: 10.1016/j.jmarsys.2014.11.001
- Pavlov, A. K., Silyakova, A., Granskog, M. A., Bellerby, R. G. J., Engel, A., Schulz, K. G., et al. (2014). Marine CDOM accumulation during a coastal Arctic mesocosm experiment: no response to elevated pCO₂ levels. *J. Geophys. Res.* 119, 1–15. doi: 10.1002/2013JG002587

- Perrette, M., Yool, A., Quartly, G. D., and Popova, E. E. (2011). Near-ubiquity of ice-edge blooms in the Arctic. *Biogeosciences* 8, 515–524. doi: 10.5194/bg-8-515-2011
- Pomeroy, L. R., and Deibel, D. (1986). Temperature regulation of bacterial activity during the spring bloom in Newfoundland coastal waters. *Science* 233, 359–361. doi: 10.1126/science.233.4761.359
- Popova, E. E., Yool, A., Aksenov, Y., and Coward, A. C. (2013). Role of advection in Arctic Ocean lower trophic dynamics: a modeling perspective. *J. Geophys. Res. Ocean.* 118, 1571–1586. doi: 10.1002/jgrc.20126
- Poulton, A. J., Daniels, C. J., Esposito, M., Humphreys, M. P., Mitchell, E., Ribas-Ribas, M., et al. (2016). Production of dissolved organic carbon by Arctic plankton communities: responses to elevated carbon dioxide and the availability of light and nutrients. *Deep Sea Res. Part II Top. Stud. Oceanogr.* 127, 60–74. doi: 10.1016/j.dsr2.2016.01.002
- Pradeep Ram, A. S., Nair, S., and Chandramohan, D. (2003). Bacterial growth efficiency in the tropical estuarine and coastal waters of Goa. Southwest Coast of India. *Microb. Ecol.* 45, 88–96. doi: 10.1007/s00248-002-3005-9
- Randelhoff, A., Fer, I., Sundfjord, A., Tremblay, J. E., and Reigstad, M. (2016). Vertical fluxes of nitrate in the seasonal nitracline of the Atlantic sector of the Arctic Ocean. *J. Geophys. Res. Oceans* 121, 5282–5295. doi: 10.1002/2016jc011779
- Randelhoff, A., Reigstad, M., Chierici, M., and Sundfjord, A. (2018). Seasonality of the physical and biogeochemical hydrography in the inflow to the Arctic Ocean through Fram strait. *Front. Mar. Sci.* 5:224. doi: 10.3389/fmars.2018.00224
- Randelhoff, A., Sundfjord, A., and Reigstad, M. (2015). Seasonal variability and fluxes of nitrate in the surface waters over the Arctic shelf slope. *Geophys. Res. Lett.* 42, 3442–3449. doi: 10.1002/2015GL063655
- Redfield, A. C. (1934). "On the proportions of organic derivations in sea water and their relation to the composition of plankton," in *James Johnstone Memorial Volume*, ed. R. J. Daniel (Liverpool: University Press of Liverpool), 176–192.
- Redfield, A. C. (1958). The biological control of chemical factors in the environment. *Am. Sci.* 46, 205–233.
- Reich, P. B., Hobbie, S. E., Lee, T., Ellsworth, D. S., West, J. B., Tilman, D., et al. (2006). Nitrogen limitation constrains sustainability of ecosystem response to CO₂. *Nature* 440, 922–925. doi: 10.1038/nature04486
- Reigstad, M., and Wassmann, P. (2007). Does *Phaeocystis* spp. contribute significantly to vertical export of organic carbon? *Biogeochemistry* 83, 217–234. doi: 10.1007/s10533-007-9093-3
- Reintaler, T., and Herndl, G. J. (2005). Seasonal dynamics of bacterial growth efficiencies in relation to phytoplankton in the southern North Sea. *Aquat. Microb. Ecol.* 39, 7–16. doi: 10.3354/ame039007
- Robinson, C. (2008). "Heterotrophic bacterial respiration," in *Microbial Ecology of the Ocean*, 2nd Edn, ed. D. L. Kirchman (Hoboken: Wiley-Black-Well), 299–334. doi: 10.1002/9780470281840.ch9
- Saba, G. K., Steinberg, D. K., and Bronk, D. A. (2011). The relative importance of sloppy feeding, excretion, and fecal pellet leaching in the release of dissolved carbon and nitrogen by *Acartia tonsa* copepods. *J. Exp. Mar. Biol. Ecol.* 404, 47–56. doi: 10.1016/j.jembe.2011.04.013
- Sakshaug, E. (2004). "Primary and secondary production in the Arctic seas," in *The Organic Carbon Cycle in the Arctic Ocean*, eds R. Stein and R. Macdonald (Berlin: Springer), 57–81. doi: 10.1007/978-3-642-18912-8_3
- Sakshaug, E., and Skjoldal, H. R. (1989). Life at the ice edge. *Ambio* 18, 60–67.
- Sambrotto, R. N., Savidge, G., Robinson, C., Boyd, P., Takahashi, T., Karl, D. M., et al. (1993). Elevated consumption of carbon relative to nitrogen in the surface ocean. *Nature* 363, 248–250. doi: 10.1038/363248a0
- Sanz-Martin, M., Chierici, M., Mesa, E., Carrillo-de-Albornoz, P., Delgado-Huertas, A., Agustí, S., et al. (2018). Episodic Arctic CO₂ limitation in the West Svalbard Shelf. *Front. Mar. Sci.* 5:221. doi: 10.3389/fmars.2018.00221
- Shen, Y., Fichot, C. G., and Benner, R. (2012). Dissolved organic matter composition and bioavailability reflect ecosystem productivity in the Western Arctic Ocean. *Biogeosciences* 9, 4993–5005. doi: 10.5194/bg-9-4993-2012
- Simon, M., and Azam, F. (1989). Protein content and protein synthesis rates of planktonic marine bacteria. *Mar. Ecol. Prog. Ser.* 51, 201–213. doi: 10.3354/meps051201
- Sipler, R. E., Gong, D., Baer, S. E., Sanderson, M. P., Roberts, Q. N., Mulholland, M. R., et al. (2017). Preliminary estimates of the contribution of Arctic nitrogen fixation to the global nitrogen budget. *Limnol. Oceanogr. Lett.* 2, 159–166. doi: 10.1002/lo2.10046
- Skoog, A., Lara, R., and Kattner, G. (2001). Spring-summer cycling of DOC, DON and inorganic N in a highly seasonal system encompassing the Northeast Water Polynya, 1993. *Deep Sea Res. Part I Oceanogr. Res. Papers* 48, 2613–2629. doi: 10.1016/s0967-0637(01)00029-2
- Sondergaard, M., Williams, P. J. L., Cauwet, G., Riemann, B., Robinson, C., Terzic, S., et al. (2000). Net accumulation and flux of dissolved organic carbon and dissolved organic nitrogen in marine plankton communities. *Limnol. Oceanogr.* 45, 1097–1111. doi: 10.4319/lo.2000.45.5.1097
- Stedmon, C. A., and Markager, S. (2001). The optics of chromophoric dissolved organic matter (CDOM) in the Greenland Sea: an algorithm for differentiation between marine and terrestrially derived organic matter. *Limnol. Oceanogr.* 46, 2087–2093. doi: 10.4319/lo.2001.46.8.2087
- Stedmon, C. A., and Nelson, N. B. (2015). "The Optical Properties of DOM in the Ocean," in *Biogeochemistry of Marine Dissolved Organic Matter*, 2nd Edn, eds D. A. Hansell and C. A. Carlson (Amsterdam: Elsevier), 481–508. doi: 10.1016/B978-0-12-405940-5.00010-8
- Strom, S. L., Benner, R., Ziegler, S., and Dagg, M. J. (1997). Planktonic grazers are a potentially important source of marine dissolved organic carbon. *Limnol. Oceanogr.* 42, 1364–1374. doi: 10.4319/lo.1997.42.6.1364
- Tameler, T., Reigstad, M., Olli, K., Slagstad, D., and Wassmann, P. (2013). New production regulates export stoichiometry in the ocean. *PLoS One* 8:e54027. doi: 10.1371/journal.pone.0054027
- Taylor, G. T., Iturriaga, R., and Sullivan, C. W. (1985). Interactions of bacterivorous grazers and heterotrophic bacteria with dissolved organic matter. *Mar. Ecol. Prog. Ser.* 23, 129–141. doi: 10.3354/meps023129
- Teira, E., Pazo, M. J., Quevedo, M., Fuentes, M. V., Niell, F. X., and Fernandez, E. (2003). Rates of dissolved organic carbon production and bacterial activity in the eastern North Atlantic Subtropical Gyre during summer. *Mar. Ecol. Prog. Ser.* 249, 53–67. doi: 10.3354/meps249053
- Thingstad, T. F., Hagstrom, A., and Rassoulzadegan, F. (1997). Accumulation of degradable DOC in surface waters: is it caused by a malfunctioning microbial loop? *Limnol. Oceanogr.* 42, 398–404. doi: 10.4319/lo.1997.42.2.0398
- Tremblay, J.-E., Michel, C., Hobson, K. A., Gosselin, M., and Price, N. M. (2006). Bloom dynamics in early opening waters of the Arctic Ocean. *Limnol. Oceanogr.* 51, 900–912. doi: 10.4319/lo.2006.51.2.0900
- Tremblay, J. É., Anderson, L. G., Matrai, P., Coupel, P., Bélanger, S., Michel, C., et al. (2015). Global and regional drivers of nutrient supply, primary production and CO₂ drawdown in the changing Arctic Ocean. *Prog. Oceanogr.* 139, 171–196. doi: 10.1016/j.pocean.2015.08.009
- Twardowski, M. S., Boss, E., Sullivan, J. M., and Donaghay, P. L. (2004). Modeling the spectral shape of absorption by chromophoric dissolved organic matter. *Mar. Chem.* 89, 69–88. doi: 10.1016/j.marchem.2004.02.008
- Van den Meersche, K., Middelburg, J. J., Soetaert, K., van Rijswijk, P., Boschker, H. T. S., and Heip, C. H. R. (2004). Carbon-nitrogen coupling and algal-bacterial interactions during an experimental bloom: modeling a C-13 tracer experiment. *Limnol. Oceanogr.* 49, 862–878. doi: 10.4319/lo.2004.49.3.0862
- Varela, M. M., Bode, A., Moran, X. A. G., and Valencia, J. (2006). Dissolved organic nitrogen release and bacterial activity in the upper layers of the Atlantic Ocean. *Microb. Ecol.* 51, 487–500. doi: 10.1007/s00248-006-9054-8
- Vernet, M., Matrai, P. A., and Andreassen, I. (1998). Synthesis of particulate and extracellular carbon by phytoplankton at the marginal ice zone in the Barents Sea. *J. Geophys. Res. Oceans* 103, 1023–1037. doi: 10.1029/97JC02288
- Vernet, M., and Whitehead, K. (1996). Release of ultraviolet-absorbing compounds by the red-tide dinoflagellate *Lingulodinium polyedra*. *Mar. Biol.* 127, 35–44. doi: 10.1007/BF00993641
- Von Stockar, U., and Liu, J. S. (1999). Does microbial life always feed on negative entropy? Thermodynamic analysis of microbial growth. *Biochim. Biophys. Acta Bioenerg.* 1412, 191–211. doi: 10.1016/S0005-2728(99)00065-1
- Walsh, J. J., McRoy, C. P., Coachman, L. K., Goering, J. J., Nihoul, J. J., Whitley, T. E., et al. (1989). Carbon and nitrogen cycling within the Bering/Chukchi Sea: source regions for organic matter affecting AOU demands of the Arctic Ocean. *Prog. Oceanogr.* 22, 277–359. doi: 10.1016/0079-6611(89)90006-2
- Wear, E. K., Carlson, C. A., James, A. K., Brzezinski, M. A., Windecker, L. A., and Nelson, C. E. (2015). Synchronous shifts in dissolved organic carbon bioavailability and bacterial community responses over the course of an

- upwelling-driven phytoplankton bloom. *Limnol. Oceanogr.* 60, 657–677. doi: 10.1002/lno.10042
- Wheeler, P. A., Watkins, J. M., and Hansing, R. L. (1997). Nutrients, organic carbon and organic nitrogen in the upper water column of the Arctic Ocean: implications for the sources of dissolved organic carbon. *Deep Sea Res. Part II Top. Stud. Oceanogr.* 44, 1571–1592. doi: 10.1016/s0967-0645(97)00051-9
- Wilson, B., Müller, O., Nordmann, E.-L., Seuthe, L., Bratbak, G., and Øvreås, L. (2017). Changes in marine prokaryote composition with season and depth over an Arctic Polar Year. *Front. Mar. Sci.* 4:95. doi: 10.3389/fmars.2017.00095
- Zubkov, M., Burkill, P. H., and Topping, J. N. (2007). Flow cytometric enumeration of DNA-stained oceanic planktonic protists. *J. Plankton Res.* 29, 79–86. doi: 10.1093/plankt/fbl059
- Zweifel, U. L. (1999). Factors controlling accumulation of labile dissolved organic carbon in the Gulf of Riga. *Estuar. Coast. Shelf Sci.* 48, 357–370. doi: 10.1006/ecss.1998.0428
- Zweifel, U. L., Norrman, B., and Hagstrom, A. (1993). Consumption of dissolved organic carbon by marine bacteria and demand for inorganic nutrients. *Mar. Ecol. Prog. Ser.* 101, 23–32. doi: 10.3354/meps101023

Conflict of Interest Statement: The authors declare that the research was conducted in the absence of any commercial or financial relationships that could be construed as a potential conflict of interest.

Copyright © 2018 Paulsen, Seuthe, Reigstad, Larsen, Cape and Vernet. This is an open-access article distributed under the terms of the Creative Commons Attribution License (CC BY). The use, distribution or reproduction in other forums is permitted, provided the original author(s) and the copyright owner(s) are credited and that the original publication in this journal is cited, in accordance with accepted academic practice. No use, distribution or reproduction is permitted which does not comply with these terms.